

Y 3.N 21/5: 6/2863

GOVT. DOC.

Dec 31 '52 BUSINESS AND
TECHNICAL DEPT.

NACA TN 2863

NATIONAL ADVISORY COMMITTEE FOR AERONAUTICS

TECHNICAL NOTE 2863

LAMINAR NATURAL-CONVECTION FLOW AND HEAT TRANSFER OF
FLUIDS WITH AND WITHOUT HEAT SOURCES IN CHANNELS
WITH CONSTANT WALL TEMPERATURES

By Simon Ostrach

Lewis Flight Propulsion Laboratory
Cleveland, Ohio



Washington

December 1952



TECHNICAL NOTE 2863

LAMINAR NATURAL-CONVECTION FLOW AND HEAT TRANSFER OF FLUIDS
WITH AND WITHOUT HEAT SOURCES IN CHANNELS WITH
CONSTANT WALL TEMPERATURES

By Simon Ostrach

SUMMARY

The natural-convection phenomenon is analyzed and it is found that the flow and heat transfer, in general, not only are functions of the Prandtl and Grashof numbers but also depend on a new dimensionless parameter. If this parameter is not negligibly small, the compression work and frictional heating may appreciably affect this mode of heat transfer.

Consideration is given to the particular case of fully developed natural-convection flow of fluids with and without heat sources between two parallel long plane surfaces the temperatures of which are maintained constant but not necessarily equal. These plates are oriented in the direction parallel to the generating body force. Solution of this problem yields detailed information on the velocity and temperature distributions and heat transfer to be expected for such flows in tall narrow channels, on the effect of heat sources in the fluid, and on the effect of frictional heating on the process. It is found that the frictional heating and the heat sources increase the velocities and temperatures within the channel formed by the two surfaces. Increasing the ratio of the two wall-temperature differences (wall minus outside ambient) also leads to similar results.

INTRODUCTION

Flows which are generated entirely by the action of body forces (such as the gravitational force) on fluids with density variations due to heating are referred to as natural- or free-convection flows. It has previously been pointed out (see reference 1, for example) that natural-convection flows are of practical importance in aeronautics. The use of natural-convection flows in hollow passages in turbine rotor blades for cooling is one of the applications of this phenomenon in

practice. With the advent of the possibility of nuclear power, the natural-convection process becomes of even greater importance, because this mode of heat transfer appears in some of the many schemes for extracting the heat energy from an atomic pile. The use of liquid metals (in which heat may also be generated by heat sources) as the heat-transfer fluid for such applications is being considered because of their suitable behavior at the high-temperature levels that would be associated with atomic power.

To date the theoretical investigations of natural-convection heat transfer have been restricted to such simple configurations as the single vertical flat plate and the horizontal cylinder. Further, the fluid considered in these investigations is usually air. The work done on more complex configurations, such as the natural-convection flow in channels or tubes, is for the most part experimental or semiempirical. An extensive experimental semiempirical study was performed by Elenbaas, who in reference 2 analyzed in an approximate manner the natural-convection heat transfer between two parallel plates heated to the same temperature and also made measurements for the case of the flow of air. In reference 3 semiempirical Nusselt numbers are compared for experiments of air flow in vertical tubes of different cross section, and in reference 4 (primarily a summary paper) functional equations for the Nusselt number are obtained by means of similarity considerations (that is, essentially by dimensional analysis). These equations are then rewritten by correlation with experimental or approximately computed results to yield semiempirical formulas for the Nusselt numbers. More recently, experimental investigations of natural-convection flows of liquid metals have been made; the results of such a study on horizontal cylinders are discussed in reference 5. None of this work on the more complex configurations yields detailed information on the velocity and temperature distributions, and it does not apply for fluids containing internal heat sources. Further, the results predicted by these semiempirical formulas deviate in some cases from the existing experimental data.

Therefore, in order to answer some of the many pending questions concerning the natural-convection flow of various fluids in enclosures and to obtain information on such flows of fluids containing heat sources, this phenomenon is analyzed herein. Particular consideration will be given to a simplified but representative case; namely, the natural-convection flow between two long parallel plates at constant temperatures oriented parallel to the direction of the generating body force. This specific problem not only retains many of the physical characteristics associated with natural-convection heat transfer but also leads to a tractable mathematical problem.

ANALYSIS

General Considerations

In general, the differential equations governing the laminar steady flow of a viscous, compressible, heat-conducting fluid which is subject to a body force are, in rectangular Cartesian tensor notation (see reference 6),

$$\frac{\partial}{\partial X_j} (\rho U_j) = 0 \quad (1)$$

$$\rho U_j \frac{\partial U_i}{\partial X_j} = \rho f_i + \frac{\partial}{\partial X_j} \left[\mu \left(\frac{\partial U_i}{\partial X_j} + \frac{\partial U_j}{\partial X_i} \right) \right] - \frac{2}{3} \frac{\partial}{\partial X_i} \left(\mu \frac{\partial U_j}{\partial X_j} \right) - \frac{\partial P}{\partial X_i} \quad (2)$$

$$\rho c_v U_j \frac{\partial T}{\partial X_j} = Q - P \frac{\partial U_j}{\partial X_j} + \frac{\partial}{\partial X_j} \left(k \frac{\partial T}{\partial X_j} \right) + \mu \left[\frac{\partial U_i}{\partial X_j} \left(\frac{\partial U_i}{\partial X_j} + \frac{\partial U_j}{\partial X_i} \right) - \frac{2}{3} \left(\frac{\partial U_j}{\partial X_j} \right)^2 \right] \quad (3)$$

$$\rho = \rho(P, T) \quad (4)$$

$$\mu = \mu(T) \quad (5)$$

and

$$k = k(T) \quad (6)$$

(A complete list of the symbols used herein is presented in appendix A.) Equations (1), (2), and (3) express, respectively, the conservation of mass, momentum, and energy; equation (4) represents a thermodynamic equation of state; and equations (5) and (6) represent the viscosity-temperature and thermal-conductivity - temperature variations. If μ and k are assumed to be constant and if the coefficient of volumetric expansion β is introduced in the body force term (see appendix B), equations (2) and (3) become

$$\rho U_j \frac{\partial U_i}{\partial X_j} = -\rho f_i \beta \theta + \mu \left[\frac{\partial}{\partial X_j} \left(\frac{\partial U_i}{\partial X_j} + \frac{\partial U_j}{\partial X_i} \right) - \frac{2}{3} \frac{\partial}{\partial X_i} \left(\frac{\partial U_j}{\partial X_j} \right) \right] - \frac{\partial P_D}{\partial X_i} \quad (2a)$$

and

$$\rho c_v U_j \frac{\partial \theta}{\partial X_j} = Q - P \frac{\partial U_j}{\partial X_j} + k \frac{\partial^2 \theta}{\partial X_j \partial X_j} + \mu \left[\frac{\partial U_i}{\partial X_j} \left(\frac{\partial U_i}{\partial X_j} + \frac{\partial U_j}{\partial X_i} \right) - \frac{2}{3} \left(\frac{\partial U_j}{\partial X_j} \right)^2 \right] \quad (3a)$$

where $P_D = P - P_s$, $\theta = T - T_s$, and the subscript s denotes a reference condition usually taken to be the hydrostatic condition.

In a manner similar to that of reference 7, equations (2a) and (3a) (neglecting heat sources) can be written in dimensionless form as

$$u_j \frac{\partial u_i}{\partial x_j} = \frac{Gr}{Re^2} \theta^* + \frac{1}{Re} \left[\frac{\partial}{\partial x_j} \left(\frac{\partial u_i}{\partial x_j} + \frac{\partial u_j}{\partial x_i} \right) - \frac{2}{3} \frac{\partial}{\partial x_i} \left(\frac{\partial u_j}{\partial x_j} \right) \right] - \frac{\partial p_D}{\partial x_i} \quad (2b)$$

and

$$\frac{1}{\gamma} u_j \frac{\partial \theta^*}{\partial x_j} = \frac{1}{Pr Re} \frac{\partial^2 \theta^*}{\partial x_j \partial x_j} - \theta_p \frac{\partial u_j}{\partial x_j} + \frac{\Theta}{Re} \left[\frac{\partial u_i}{\partial x_j} \left(\frac{\partial u_i}{\partial x_j} + \frac{\partial u_j}{\partial x_i} \right) - \frac{2}{3} \left(\frac{\partial u_j}{\partial x_j} \right)^2 \right] \quad (3b)$$

by letting $u_i = U_i / \bar{U}$, $\theta^* = \theta / \theta_w$, $x_i = X_i / d$ and $p = P / \rho \bar{U}^2$. Here, \bar{U} should denote a unique velocity which characterizes the flow, and in the case of forced-convection flows this is taken to be the prescribed reference velocity U_∞ (as for example, the free-stream velocity). From equations (2b) and (3b) it can then be seen that the solutions of the dynamic and thermodynamic problems for the forced-convection flow (at velocity U_∞), taking into account also the body force action, are given in terms of four parameters; namely, the Grashof number Gr , the Reynolds number Re , the Prandtl number Pr , and the dimensionless temperature number Θ . The parameter Θ is defined

$$\Theta = \frac{U_\infty^2}{c_p(T_w - T_s)} = 2 \frac{\theta_a}{\theta_w}$$

and it is argued that if $U_\infty^2 \ll c_p(T_w - T_s)$ or, equivalently, if $\theta_a \ll \theta_w$, then the compression work and frictional dissipation terms (the last two terms, respectively, in equation (3b)) can be neglected with respect to the conduction and convection. For the case of pure natural-convection flows, there exists no unique prescribed characteristic velocity U_∞ , so that the parameter Θ as well as the Reynolds number Re becomes meaningless. Equations (1), (2a), and (3a) still hold, but now instead of using U_∞ as a reference velocity to obtain dimensionless equations, some group of the physical quantities (such as f_X , θ_w , and β) which are directly connected with the natural-convection phenomenon must be utilized. Such a group was found in references 1, 2, and 8 to be

$$\bar{U} = \frac{f_X \beta \theta_w d^2}{\nu} \quad (7)$$

(For convenience, f_X is here taken to be the negative of the X -component of the body force per unit mass.) Hence, with this expression for \bar{U} as the reference velocity, the dimensionless forms of the momentum and energy equations for the case of natural-convection flow are

$$u_j \frac{\partial u_i}{\partial x_j} = \frac{\theta^*}{Gr} + \frac{1}{Gr} \left[\frac{\partial}{\partial x_j} \left(\frac{\partial u_i}{\partial x_j} + \frac{\partial u_j}{\partial x_i} \right) - \frac{2}{3} \frac{\partial}{\partial x_i} \left(\frac{\partial u_j}{\partial x_j} \right) \right] - \frac{\partial p_D}{\partial x_i} \quad (2c)$$

and

$$\frac{1}{\gamma} u_j \frac{\partial \theta^*}{\partial x_j} = \frac{1}{Pr Gr} \frac{\partial^2 \theta^*}{\partial x_j \partial x_j} - Gr \frac{\beta f_X d}{c_p} p \frac{\partial u_j}{\partial x_j} + \frac{\beta f_X d}{c_p} \left[\frac{\partial u_i}{\partial x_j} \left(\frac{\partial u_i}{\partial x_j} + \frac{\partial u_j}{\partial x_i} \right) - \frac{2}{3} \left(\frac{\partial u_j}{\partial x_j} \right)^2 \right] \quad (3c)$$

Setting $Gr \frac{\beta f_X d}{c_p} = \bar{K}$, equation (3c) can be written as

$$\frac{1}{\gamma} u_j \frac{\partial \theta^*}{\partial x_j} = \frac{1}{Pr Gr} \frac{\partial^2 \theta^*}{\partial x_j \partial x_j} - \bar{K} p \frac{\partial u_j}{\partial x_j} + \frac{\bar{K}}{Gr} \left[\frac{\partial u_i}{\partial x_j} \left(\frac{\partial u_i}{\partial x_j} + \frac{\partial u_j}{\partial x_i} \right) - \frac{2}{3} \left(\frac{\partial u_j}{\partial x_j} \right)^2 \right] \quad (3d)$$

The new dimensionless group $\beta f_X d / c_p$ which appears here was first encountered in the analysis of reference 9. It does not appear explicitly in that reference, however, since for the particular case considered it was approximated by $\rho g d / P$ by means of the state equation for a gas, and this last expression was negligibly small. This group was also obtained in reference 5 by a formal dimensional analysis, but its physical significance and function were not discussed. By comparison of equations (2c) and (3d) with (2b) and (3b) it can be seen that for the case of pure natural-convection flow the Grashof number is analogous to the Reynolds number for forced flows and the factor \bar{K} is analogous to the dimensionless temperature number θ . In fact, Gr and \bar{K} are, respectively, simply Re and θ based on \bar{U} as given in equation (7). Therefore, for pure natural-convection flows the influence of the compression work and frictional dissipation terms in the energy equation should be determined by the parameter \bar{K} and not by θ . Previously, the effects of the compression work and frictional heating had been neglected in the natural-convection phenomenon on the basis of qualitative arguments showing that θ was always small; in order to do so a guess had to be made of the value of the reference velocity. Since it has here been demonstrated that \bar{K} , and not θ , is critical in determining the influence of the compression work and frictional heating on the flow and heat transfer in the purely natural-convection process, it must be determined whether in actual

practice \bar{K} is always negligibly small. If \bar{K} is always very small, then, of course, there would be no need to extend the previous work in this respect. However, calculations show that even under relatively mild conditions, moderately large values of \bar{K} are possible. When it is further realized that the three prime physical factors in the natural-convection process, f_X , β , and θ_w , appear in the numerator of the expression for \bar{K} and that in the more recent applications these could easily be many times those values usually associated with this mode of heat transfer (for example, f_X could be as much as 10^5 g in a centrifugal field, and β and θ_w also could be much larger in atomic energy applications), it becomes clear that in many practical cases the compression work and frictional heating will influence the natural-convection flow and heat transfer.

An interesting and different characteristic of the natural-convection phenomenon becomes evident if the compression work and frictional heating are taken into consideration. In this case, for example, the frictional heating is added to the physically imposed heat and should act as a heat source in the fluid and, hence, tend to increase the flow velocities.

Specific Problem

To solve the system of equations governing the natural-convection flow and heat transfer would at best be a formidable task because of the nonlinearity of the equations and because of the interrelation of the equations of motion with the energy equation. The consideration of the compression work and frictional heating terms in the energy equation makes the problem still more complicated. Therefore, in order to obtain equations which are tractable mathematically, it is necessary to make some simplifying assumptions. In this report, therefore, consideration is given to a simplified configuration which leads to less complicated equations but which, nevertheless, retains the essential physical behavior of the natural-convection process. In this way detailed velocity and temperature distributions can be computed, and the effects of heat sources and of frictional heat can be studied.

Fully developed flow between long parallel plates with constant wall temperature. - The simplified configuration to be studied is the fully developed laminar natural-convection flow between two long parallel plane surfaces or plates which are oriented in the direction of the generating body force (see fig. 1) and which are open at the ends to the ambient fluid. The surface temperatures are constant, but one surface may be at a different temperature from the other. For such a configuration it is assumed that the velocity, as in the more

familiar Poiseuille flow case, and temperature depend only on the transverse coordinate Y . The simultaneous assumption of these two conditions implies that there is always a net heat flow to the walls and also that the transverse velocity component V vanishes identically. Under these conditions equation (1) is identically satisfied, and the system of equations (2a) and (3a) becomes

$$\frac{d^2U}{dY^2} + \frac{\beta \rho f_X}{\mu} \theta - \frac{\partial P_D}{\partial X} = 0 \quad (8)$$

$$\frac{\partial P_D}{\partial Y} = 0 \quad (9)$$

and

$$\frac{d^2\theta}{dY^2} + \frac{\mu}{k} \left(\frac{dU}{dY} \right)^2 + \frac{Q}{k} = 0 \quad (10)$$

where now the more familiar notation $U_1 = U$, $U_2 = V$, $X_1 = X$ and $X_2 = Y$ is used. The product $\beta \rho$ in the coefficient $\beta \rho f_X / \mu$ in equation (8) can be written as N for fluids, as is discussed in appendix B. For gases, the density ρ can always be combined with the absolute viscosity μ to form the kinematic viscosity ν , and ν should be evaluated at some convenient and representative reference point (as, for example, at the average of the wall temperatures).

By equation (9), P_D is seen to be a function of X alone. Since U and θ have been assumed to be functions of Y alone, it is evident from equation (8) that dP_D/dX must be a constant. Hence the pressure gradient dP/dX inside the channel differs from the hydrostatic pressure gradient by at most a constant, since

$$\frac{dP}{dX} = \frac{dP_S}{dX} + \frac{dP_D}{dX} = \frac{dP_S}{dX} + \text{constant}$$

However, the pressure difference required to accelerate the fluid from the hydrostatic to the fully developed condition and the pressure difference to decelerate it back to the hydrostatic condition must be finite. Therefore, since the channel is assumed very long, the pressure gradient inside the channel becomes equal to the hydrostatic pressure gradient, and equation (8) may be written as

$$\frac{d^2U}{dY^2} + \frac{\beta \rho f_X}{\mu} \theta = 0 \quad (8a)$$

At this point several interesting observations can be made concerning equations (8a) and (10). First of all, in equation (8a) as in the forced Poiseuille flow equation, the inertia terms (left side of equation (3c)) vanish, but now the driving (buoyancy) term (second term in equation (8a)) is a function of the transverse coordinate; whereas, in forced Poiseuille flow the driving term (pressure gradient) is a function of the longitudinal coordinate.

If the frictional heating term (second in equation (7)) is neglected, the energy equation is independent of the velocity distribution, but the equation of motion, which yields the velocity, is dependent on the temperature. This state of affairs is the opposite of that occurring in the forced-convection Poiseuille flow. Also, the convection and compression work terms in the energy equation (3a) now vanish. Although these last effects are eliminated, the solution of this simplified problem should not only yield practical results for the natural-convection flows in tall-narrow channels but should also show the effect of heat sources in the fluid (last term in equation (10)) and the effect of frictional heating (second term in equation (10)) on the natural-convection process.

The boundary conditions associated with this problem are as follows: the fluid must adhere to the walls of the channel (the no-slip condition of viscous fluids) or, mathematically,

$$U(0) = U(d) = 0$$

and the temperature of the fluid at the plate must equal the plate temperature, or

$$\theta(0) = T_{w0} - T_s \equiv \theta_{w0}$$

and

$$\theta(d) = T_{w1} - T_s \equiv m\theta_{w0} \equiv \theta_{w1}$$

Let

$$U = (\bar{U}/K)u = (k/f_X \beta \rho d^2)u = \sqrt{\frac{c_p \theta_{w0}}{K \Pr}} u$$

$$Y = yd$$

and

$$\theta = (k \mu / f_X^2 \beta^2 \rho^2 d^4) \tau = \frac{\theta_{w0}}{K} \tau$$

Equations (8a) and (10) become

$$u'' + \tau = 0 \quad (11)$$

$$\tau'' + (u')^2 + \alpha K = 0 \quad (12)$$

where $\alpha = Qd^2/k\theta_{w0}$ and $K = \text{Pr} \bar{K} = \text{Pr} \text{Gr} \frac{\beta f_X d}{c_p}$ and the primes denote differentiation with respect to y .

The boundary conditions are

$$u(0) = u(1) = 0$$

$$\tau(0) = K$$

and

$$\tau(1) = mK$$

where $m = \theta_{w1}/\theta_{w0}$.

It is interesting that in this particular problem it is necessary to have a priori information on three temperatures (T_s , T_{w0} , and essentially T_{w1}) in order to determine the actual temperature distribution, and that these appear explicitly only as the ratio of two temperature differences in the analysis. Combination of equations (11) and (12) to eliminate the dependent variable τ yields

$$u^{iv} - (u')^2 - \alpha K = 0 \quad (13)$$

with the boundary conditions

$$u(0) = u(1) = 0$$

$$u''(0) = -K \quad (14)$$

and

$$u''(1) = -mK$$

For convenience, the heat-source distribution is taken to be uniform, so that Q and hence α are constants. The method of solution to be described is in no way dependent upon this restriction; that is, Q and α could be functions of the independent variable, and the same method could be applied in principle. In order to solve the given boundary value problem (equations (13) and (14)) a method

of successive approximations is employed. The equation for this technique can be written

$$u_r^{iv} - [u'(r-1)]^2 - \alpha K = 0 \quad (15)$$

where $r = 0, 1, \dots$ denotes the order of the approximation and where $u'_{-1} \equiv 0$ by definition. It should be noted that $r = 0$ yields the same equation as would apply when the frictional heating is neglected. By elementary quadratures the zeroth-order ($r = 0$) approximation u_0 is

$$u_0 = K \sum_{i=1}^4 \frac{a_i}{i!} y^i \quad (16)$$

where

$$a_1 = \frac{1}{24} (4m + \alpha + 8)$$

$$a_2 = -1$$

$$a_3 = - \left(m + \frac{\alpha}{2} - 1 \right)$$

$$a_4 = \alpha$$

and from equation (11)

$$\tau_0 = -u_0''' = -K \sum_{i=2}^4 \frac{a_i}{(i-2)!} y^{(i-2)} \quad (17)$$

The next higher approximation (considering now frictional heating) is

$$u_1 = u_0 + \frac{K^2}{576(2520)} \sum_{i=1}^{10} \bar{a}_i y^i \quad (18)$$

where

$$\bar{a}_1 = 35\alpha^2 + 320m\alpha + 328\alpha + 792m^2 + 1392m + 840$$

$$\bar{a}_2 = 0$$

$$\bar{a}_3 = -2(51\alpha^2 + 444m\alpha + 564\alpha + 1008m^2 + 2352m + 1680)$$

$$\bar{a}_4 = 105(4m + \alpha + 8)^2$$

$$\bar{a}_5 = -1008(4m + \alpha + 8)$$

$$\bar{a}_6 = -84(\alpha^2 + 6m\alpha + 6\alpha + 8m^2 + 8m - 64)$$

$$\bar{a}_7 = 24(\alpha^2 + 4m\alpha + 44\alpha + 72m - 72)$$

$$\bar{a}_8 = 18(3\alpha^2 + 12m\alpha - 28\alpha + 12m^2 - 24m + 12)$$

$$\bar{a}_9 = -80\alpha \left(m + \frac{\alpha}{2} - 1 \right)$$

$$\bar{a}_{10} = 8\alpha^2$$

and

$$\tau_1 = \tau_0 - \frac{K^2}{576(2520)} \sum_{i=3}^{10} i(i-1) \bar{a}_{i-2} y^{(i-2)} \quad (19)$$

Equations (16) and (17) yield the velocity and temperature distributions, neglecting the frictional heating; and equations (18) and (19) hold for small but significant values of K and, hence, show the effect of considering the frictional heating to a first approximation. To obtain solutions for somewhat larger K , it would be necessary to continue with the iterative procedure described previously to obtain the higher-order approximations. Such a scheme becomes extremely tedious, and, furthermore, the convergence of the method can be established by comparison with a direct numerical solution of the complete boundary-value problem (equations (13) and (14)). Some discussion of these numerical results relative to the solutions given by equations (16) to (19) will be presented herein, and a more complete and detailed account of the numerical results together with a detailed account of the numerical solution procedure used is in progress. Comparison of these solutions obtained from equations (18) and (19), in which the frictional heating is considered to a first approximation, to the numerical solutions, in which the frictional heating is completely accounted for, should indicate the range of applicability and accuracy of equations (18) and (19).

RESULTS AND DISCUSSION

Velocity and Temperature Distributions

The relations between the actual and dimensionless velocities and temperatures as determined from the various transformations in the analysis are

$$U \sqrt{\frac{K \Pr}{c_p \theta_{w0}}} = u \quad (20)$$

and

$$K \frac{\theta}{\theta_{w0}} = \tau \quad (21)$$

where U and θ denote the actual, and τ and u denote the dimensionless quantities. For a given heat-transfer fluid and configuration (as specified through K and m) and for a given heat-source intensity (as specified through α) the dimensionless velocity and temperature distributions in equations (20) and (21) can be computed from equations (16) to (19). These computations will be accurate within the limits of the method of solution; that is, for small K . For larger K , computations of u and τ can best be determined by direct numerical solution of equations (13) and (14). The range of applicability of the solutions given by equations (16) to (19) will be discussed more fully subsequently. Representative velocity and temperature distributions were calculated for values of $K = 0.5$, 3.0, and 10.0.

The particular values of ratio of wall-temperature differences m chosen for the computations correspond to the following interesting cases: (1) $m = -1$, in which the arithmetic average of the wall temperatures is equal to the temperature of the ambient fluid (that is, $(T_{w1} + T_{w0})/2 = T_s$); (2) $m = 0$, in which one wall is at the reservoir or ambient temperature; (3) $m = 1$, in which both walls are at the same temperature, and, hence, the effect of the wall-temperature difference is eliminated; and (4) $m = 2$, in which the wall temperatures are unequal but both are maintained at higher or lower temperatures than the ambient.

Combinations of K and m used in the computations and the figure in which the results are plotted are given in the following table:

K	0.5	0.5	0.5	0.5	3.0	3.0	3.0	3.0	10.0	10.0	10.0	10.0
Ratio of wall-temperature differences, m	-1	0	1	2	-1	0	1	2	-1	0	1	2
Velocity-profile figure number	2(a)	2(b)	2(c)	2(d)	3(a)	3(b)	3(c)	3(d)	4(a)	4(b)	4(c)	4(d)
Temperature-profile figure number	5(a)	5(b)	5(c)	5(d)	6(a)	6(b)	6(c)	6(d)	7(a)	7(b)	7(c)	7(d)

2670
 For each K and m combination profiles were calculated for $\alpha = 0$, 10, and 100 with frictional heating neglected (given by equations (16) and (17) and denoted by u_0 and τ_0 on the figures), with frictional heating included to a first approximation (given by equations (18) and (19) and denoted by u_1 and τ_1), and, in several specific cases, with frictional heating completely accounted for (given by the numerical solution of equations (13) and (14) and denoted by u and τ).

The computed results presented herein pertain specifically to a configuration wherein the body force is acting in the negative X -direction and at least one wall temperature is always greater than the ambient (that is, $T_w > T_s$).

Effect of different wall-temperature configurations (m varying) and heat sources (α varying). - Examination of typical cases in figures 2 to 7 shows that, as expected, an increase in the heat-source parameter α or an increase in the wall-temperature parameter m results in larger velocities and higher temperatures. The velocity profiles change in such a way that the net mass through-flow, as represented essentially by the area under the u -curves, increases with m and α from zero at $m = -1$ and $\alpha = 0$. The velocity profiles become more symmetric with increasing α , and for $\alpha = 0$, negligible frictional heating, and $m = 1$, the profiles are similar to the Poiseuille profiles. For any given set of conditions, a decrease in the net mass through-flow or even no net mass through-flow can, of course, be obtained by adjusting the wall-temperature ratios so that m takes on larger negative values. It can also be seen from the temperature distributions that, as previously predicted, in all cases considered, either heat is being transferred to both walls or heat is flowing from one wall out through the other. For the case of no heat sources in the fluids and neglecting frictional heating, the temperature distributions, as are to be expected, are just the conduction profiles.

Effect of frictional heating. - The effect of frictional heating can be seen in figures 2 to 7 by comparing the curves computed by neglecting frictional heating (denoted by subscript zero) with those computed by including frictional heating as a first approximation (denoted by subscript unity) for a given set of conditions. Numerical solutions of equations (13) and (14) obtained for several specific sets of conditions are also included (with no subscripts) for comparison with the approximate solutions. For $K = 0.5$ and all α and m considered, the frictional heating effect is small; that is, the u_1 and τ_1 and u and τ curves are not appreciably different from the u_0 and τ_0 curves, respectively. However, even for

values of K relatively near unity, as is here represented by the case $K = 3$, there are conditions of m and α in which the frictional heating begins to alter the results appreciably. This situation could, depending on m and α , also occur for even lower values of K . In fact there are many combinations of K , m , and α for which the frictional heating becomes important. For example, the deviation between the solutions neglecting frictional heating (denoted by subscript zero) and those including the frictional heating to a first approximation (denoted by subscript unity) for the case $\alpha = 0$ first become marked for $K = 10$ and $m = 1$ (see figs. 4(c) and 7(c)). This deviation is more pronounced the higher the value of K for given m and α . As was previously stated, moderately large values of K (or \bar{K}) can be obtained under relatively mild conditions. For example, for the natural-convection flow of air under the influence of gravity at room temperature, with θ_w equal to 1000° R and the Grashof number equal to 10^7 , K is approximately 12.1 ($\bar{K} = 16.8$); for the flow of water in a gravitational field with θ_w of 150° R and a Grashof number of 10^8 , K is approximately 26.1 ($\bar{K} = 3.7$). From the specific computations made herein, it can be seen that for $\alpha = 10$, the deviation mentioned previously first becomes apparent for $K = 3$ and $m = 2$ (see figs. 3(d) and 6(d)); and for $\alpha = 100$, a large difference exists for $K = 3$ and $m = -1$ (figs. 3(a) and 6(a)). Hence, on the basis of the computations presented herein, it can roughly be stated that the solutions as given by equations (16) and (17) will be sufficiently accurate up to the limits previously stated. Beyond these limits the solutions including frictional heating effects to a first order (equations (18) and (19)) should be used. It should be kept in mind, however, that more detailed computations are necessary to define these limits more precisely.

Numerical solutions which completely include the frictional heating effects and which are denoted by u and τ without subscripts are also presented in the figures only for the cases of (K, m, α) of $(3, -1, 0)$, $(3, 1, 0)$, $(10, -1, 0)$, $(10, 1, 0)$, $(10, 2, 0)$, $(3, 1, 10)$, $(3, 1, 100)$, and $(10, 2, 10)$ in order to show the relative accuracy of the u_1 and τ_1 solutions. For most of these cases, these numerical solutions coincide with the u_1 and τ_1 solutions; but in the higher internal-heat-generation cases (as given by high K , m , and α), these two sets of solutions differ (see figs. 3(c), 6(c), 4(d), and 7(d)). A significant difference indicates that the u_1 and τ_1 solutions, as given by equations (18) and (19), respectively, are not sufficiently accurate. For the range of values of K , m , and α computed here, it appears that equations (18) and (19) could well be used for $\alpha = 0$ for all K and m in this range, for $\alpha = 10$ up to values of $K = 10$ and $m = 2$ (figs. 4(d) and 7(d)), and for $\alpha = 100$ up to $K = 3$ and $m = 1$ (figs. 3(c) and 6(c)). Beyond these limits, equations (18) and (19) lose their accuracy, and the complete numerical solutions of equations (13) and (14) should be used.

The consideration of frictional heating not only changes the shape of the temperature profiles but also leads to flows with increased velocities, as was expected. This change of temperature profile appreciably alters the temperature gradients at the walls and hence the heat transfer.

In addition to these trends, the consideration of frictional heating leads to other interesting results. These results, which were obtained in computing the numerical solutions which completely take into account the frictional effects, are that two solutions exist for a given set of conditions and that there exists a critical set of conditions beyond which no solutions exist. Physically, the presence of two solutions predicts the existence of two heat-transfer and flow states for a given set of conditions, which appears to be a situation analogous to that in a Laval nozzle. The existence of critical conditions appears to be similar to the thermal-choking phenomenon. One of the two flow states mentioned (the one encountered first physically) corresponds, as is seen in the figures, to the u_1 and τ_1 solutions (or, more accurately, the u and τ solutions); but the other, computed here only for the case of $K = 10$, $m = 2$, and $\alpha = 0$, denoted by the curves labeled $u^{(2)}$ and $\tau^{(2)}$ on figures 4(d) and 7(d), represents velocities and temperatures many times larger than the others at the same conditions. These results are being further investigated.

Actual values of the velocities and temperatures can be computed from equations (20) and (21) and figures 2 to 7. Since so many factors appear in those expressions, it is clear that there is considerable freedom in choosing the fluid and the physical conditions to obtain almost any given flow and heat transfer. For example, if $Gr = 2 \times 10^6$, $f_X = 6g$, and $\theta_{w0} = 100^\circ R$ for air at standard room conditions

($T_s = 500^\circ R$), a maximum velocity of 382 feet per second and a maximum temperature of almost $700^\circ R$ would be obtained with both walls at the same temperature (that is, $m = 1$). These conditions could very easily be obtained in an extremely mild centrifugal force field.

For such computations to have quantitative significance, it should be kept in mind that this analysis pertains only to laminar flows. It is not possible to state under what conditions the transition from laminar to turbulent flow will occur, because no general stability theory exists for natural-convection flows. The only available natural-convection stability information is the experimental result indicated in reference 10 that transition on a single vertical plate occurs at a Grashof number of approximately 10^9 . (All values of Gr used in the numerical examples herein were less than 10^9 .) There is, in fact, relatively little general stability information for forced-convection channel flow with heat transfer, so that it is not even possible to obtain a rough transition criterion by relating the present problem to an equivalent forced-convection problem.

Although computations are presented herein only for a particular configuration, the analysis itself and the approximate solutions given by equations (16) to (19) are in no way limited to a single configuration. A change only in the body force direction (sign) merely alters the flow direction; that is, the sign of the velocity changes, or, in mathematical terminology, the velocity is an odd function of the body force. If there are no heat sources in the fluid and the effects of frictional heating are negligible, a change in the surface thermal condition (say, from $T_w > T_s$ to $T_w < T_s$) would also result in a change in flow direction. However, when either heat sources are present or frictional heating is not negligible, or both, the anti-symmetry with respect to θ_w is disrupted. For the case $T_w > T_s$, the internal heat (due to heat sources or friction) increases the flow in a given direction as is shown in figures 2 to 4; but for $T_w < T_s$, this heat tends to retard the flow in a given direction and, if large enough, can change the flow direction. These effects can be seen in figure 8, where the velocity distributions are presented for a representative case ($K = 10$, $m = 2$, $\alpha = 0, 10, 100$) where $T_w < T_s$. The associated temperature profiles are given in figure 9. Frictional heating is appreciable for $\alpha = 0$ and 100 but not for $\alpha = 10$; and although for $\alpha = 100$ the flow is again in the same direction as for the same case for $T_w > T_s$ (fig. 4(d)), the velocities are smaller for $T_w < T_s$.

Unfortunately, there are no experimental results available with which to compare the results predicted herein. The experiments of Elenbaas (reference 2) were made with short plates, and, consequently, there were variations of velocity and temperature profiles with the longitudinal distance. Such variations were not considered in this analysis.

Heat Transfer

The heat-transfer coefficients for the natural-convection process considered here can be expressed in terms of Nusselt numbers. For the case where the walls are not at the same temperature (that is, $m \neq 1$),

$$Nu \equiv \frac{hd}{k} = \left(\frac{dT}{dY} \right)_{0,d} \frac{d}{(T_{w1} - T_{w0})}$$

where the double subscript $0,d$ signifies that the temperature gradient is to be evaluated at either $Y = 0$ or $Y = d$, depending on which wall is under consideration. By means of the various transformations in the analysis this expression can be written

$$Nu = \frac{1}{(m-1)K} \left(\frac{d\tau}{dy} \right)_{0,1}$$

By use of equation (19), the Nusselt number for the wall at $y = 0$ is

$$Nu_0 = \frac{1}{(m-1)} \left[m + \frac{\alpha}{2} - 1 + \frac{K}{48(2520)} (51\alpha^2 + 444m\alpha + 564\alpha + 1008m^2 + 2352m + 1680) \right]$$

and for the wall at $y = 1$

$$Nu_1 = \frac{1}{(m-1)} \left[m - \frac{\alpha}{2} - 1 - \frac{K}{48(2520)} (51\alpha^2 + 564m\alpha + 444\alpha + 1680m^2 + 2352m + 1008) \right]$$

The Nusselt numbers were computed from these expressions over a range of values of K for $m = -1, 0$, and 2 , and $\alpha = 0, 10$, and 100 , and are presented in figures 10 and 11. In general, the Nusselt numbers increase with increasing K , m , and α . Comparison of figures 10 and 11 shows that for $m = -1$ the Nusselt numbers for the wall at $y = 1$ are larger than for the wall at $y = 0$. However, as m increases to 2 , this result is reversed.

When the walls are at the same temperature ($m = 1$) the Nusselt number can be written as

$$Nu = \left(\frac{dT}{dY} \right)_0 \frac{d}{\theta_w}$$

and from the transformations in the analysis, this equation becomes

$$Nu = \frac{1}{K} \left(\frac{d\tau}{dy} \right)_0$$

Again from equation (19)

$$Nu = \left[\frac{\alpha}{2} + \frac{K}{48(2520)} (51\alpha^2 + 1008\alpha + 5040) \right]$$

The Nusselt numbers computed for this case are presented in figure 12.

CONCLUSIONS

An analysis of the natural-convection phenomenon shows that the flow and heat transfer not only are functions of the Prandtl and Grashof numbers but also depend upon a new dimensionless factor, \bar{K} . For values of \bar{K} which are not negligible, the frictional heating and compression work may appreciably alter the results. Consideration was given to the particular simplified case of the fully developed natural-convection flow of fluids with and without heat sources between two long parallel surfaces oriented in the direction parallel to the generating body force. These surfaces were taken to have constant but not necessarily equal temperatures. The velocity and temperature distributions for this special case were determined, and it was observed that increasing the wall-temperature ratio increased the flow velocities, the net mass through-flow, and the temperatures. The effect of the heat sources was also found to increase velocities, temperatures, and mass flows. The frictional heating appreciably altered the velocity and temperature profiles in some cases, showing that the velocities were increased and the heat transfer at the walls was greatly changed by this effect. Consideration of the frictional heating also led to the prediction of two flow and heat-transfer states for a given set of conditions and to a critical set of conditions beyond which no solutions existed. These last two results are being more completely investigated.

Lewis Flight Propulsion Laboratory
National Advisory Committee for Aeronautics
Cleveland, Ohio, October 6, 1952

APPENDIX A

SYMBOLS

The following notation is used in this report:

a_i, \bar{a}_i	coefficients in successive approximation solutions
c_p	specific heat at constant pressure
c_v	specific heat at constant volume
d	characteristic length (specifically distance between plates)
f_i	components of body force per unit mass, $i = 1, 2, 3, \dots$
f_X	negative of X -component of body force per unit mass
Gr	Grashof number, $\frac{\beta f_X \theta_w d^3}{\nu^2}$
g	gravitational force per unit mass (or acceleration due to gravity)
h	heat-transfer coefficient
K	dimensionless parameter, $\Pr \text{Gr} \frac{\beta f_X d}{c_p}$
\bar{K}	dimensionless parameter, K/\Pr
k	thermal-conductivity coefficient
m	ratio of wall-temperature differences, $T_{w1} - T_s / T_{w0} - T_s$
N	a constant
Nu	Nusselt number
P	pressure
P_D	$P - P_s$
P_s	hydrostatic pressure

Pr	Prandtl number
p	dimensionless pressure
Q	heat added by heat sources
Re	Reynolds number
T	temperature
U	longitudinal velocity component
\bar{U}	characteristic reference velocity
U_i	velocity components, $i = 1, 2, 3, \dots$
U_∞	prescribed reference velocity in forced-convection flow
u	dimensionless longitudinal velocity component
u_i	dimensionless velocity components, $i = 1, 2, 3, \dots$
V	transverse velocity component
X_i	rectangular Cartesian coordinates, $i = 1, 2, 3, \dots$
x_i	dimensionless coordinates, $i = 1, 2, 3, \dots$
Y	coordinate
y	dimensionless coordinate
α	dimensionless heat-source parameter, $Qd^2/k\theta_w$
β	coefficient of volumetric expansion, $\rho \left[\frac{\partial(1/\rho)}{\partial T} \right]_P$
γ	ratio of specific heats
Θ	dimensionless temperature number, $U_\infty^2/c_p \theta_w$
θ	$T - T_s$
θ^*	dimensionless temperature difference, θ/θ_w

2670

μ absolute viscosity coefficient
 ν kinematic viscosity coefficient
 ρ density
 τ dimensionless temperature

Subscripts:

a denotes adiabatic condition
 i, j rectangular Cartesian tensor and summation subscripts
 r successive approximation subscript
 s denotes a reference condition (usually taken as the hydrostatic condition)
 w denotes wall conditions
 w_0 denotes condition at $y = 0$
 w_1 denotes condition at $y = 1$

Superscripts:

(2) denotes second flow and heat-transfer state

APPENDIX B

DERIVATION OF BUOYANCY TERM

It is often convenient in natural-convection studies to express the body force term (first term on right side of equation (2)) as a buoyancy term. To this end, the case is considered in which the surface (specifically here, the channel) and the fluid are at the same temperature and there is no flow. Equation (2) then becomes

$$\rho_s f_i - \frac{\partial P_s}{\partial x_i} = 0 \quad (B1)$$

where the subscript s indicates the hydrostatic condition, and equation (B1) then expresses the fact that under this condition the body force is in equilibrium with the hydrostatic pressure gradient. This equilibrium is, of course, upset if there is a temperature variation in the flow field, and the unbalanced force, which is the buoyancy force, causes a flow to be established. In order to introduce the buoyancy term into the equation, the body force and pressure terms in equation (2)

$$\rho f_i - \frac{\partial P}{\partial x_i}$$

can be written

$$\rho_s f_i + (\rho - \rho_s) f_i - \frac{\partial P_s}{\partial x_i} - \frac{\partial P_D}{\partial x_i}$$

where $P_D = P - P_s$.

Hence, in view of equation (B1), these terms become

$$(\rho - \rho_s) f_i - \frac{\partial P_D}{\partial x_i} \quad (B2)$$

The pressure gradient in the preceding expression appears in just that form in equation (2a), but now the buoyancy term is to be expressed in terms of a temperature difference. It is first assumed that the density is a function of temperature alone, so that equation (4) can be written

$$\rho = \rho(T) \quad (B3)$$

In the case of a liquid, this assumption is evident; whereas, in the case of a gas, it implies that the pressure changes are small as compared with the absolute pressure. If the coefficient of volumetric expansion β is introduced, equation (B3) can be written

$$d\rho = -\beta \rho dT \quad (B4)$$

The writing of the density difference in expression (B2) in terms of a temperature difference can now be effected in one of several ways, depending on the specific problem.

Most of the theoretical work done to date applies only for the case of small temperature differences. Hence, for that case the differentials in equation (B4) are replaced by differences to yield

$$\beta = \frac{1}{\rho} \frac{(\rho - \rho_s)}{(T_s - T)}$$

The buoyancy term in equation (B2) then becomes

$$(\rho - \rho_s) f_i = -\rho f_i \beta (T - T_s) \quad (B5)$$

as it appears in equation (2a).

If the analysis is not to be limited to the case of small temperature differences, equation (B5) can be obtained in either of the following ways, depending on whether the fluid is a liquid or a gas. For liquids, it is assumed that $\beta \rho = N$ where N is a constant. A numerical check of this assumption shows that it is reasonable under commonly encountered conditions for most fluids; in particular, if the constant is evaluated at the ambient condition, the variation of $\beta \rho$ over a large range of temperature is small. (For unusually large temperature ranges N could be evaluated at some other appropriate condition.) As a result of this assumption a linear density-temperature variation is obtained from equation (B4), and then by direct substitution equation (B5) is obtained. For gases, the equation of state is

$$P = \rho R T \quad (B6)$$

where R is the gas constant.

Substitution into the buoyancy term yields

$$(\rho - \rho_s) f_i = \frac{P}{RT} \left[1 - \frac{P_s}{P} \frac{T}{T_s} \right] f_i$$

It need now only be assumed that the difference between P and P_s is everywhere small; therefore

$$(\rho - \rho_s) f_i = \frac{\rho f_i}{T_s} (T_s - T) \quad (B7)$$

By definition, $\beta = 1/T$ for gases, so that the final desired form

$$(\rho - \rho_s) f_i = - \rho f_i \beta_s (T - T_s)$$

is obtained. In this case, β is evaluated at the hydrostatic condition. An equivalent form could also be obtained where the density would be evaluated at that condition and β could be variable.

REFERENCES

1. Ostrach, Simon: An Analysis of Laminar Free-Convection Flow and Heat Transfer About a Flat Plate Parallel to the Direction of the Generating Body Force. NACA TN 2635, 1952.
2. Elenbaas, W.: Heat Dissipation of Parallel Plates by Free Convection. *Physica*, vol. IX, no. 1, Januari 1942, pp. 1-28.
3. Elenbaas, W.: The Dissipation of Heat by Free Convection - The Inner Surface of Vertical Tubes of Different Shapes of Cross-Section. *Physica*, vol. IX, no. 8, Sept. 1942, pp. 865-874.
4. Elenbaas, W.: Dissipation of Heat by-Free Convection. *Philips Res. Rep.*, pt. I, vol. 3, 1948, pp. 338-360; pt. II, vol. 3, pp. 450-465.
5. Hyman, Seymour C., Bonilla, Charles F., and Ehrlich, Stanley W.: Natural Convection Processes. I - Heat Transfer to Liquid Metals and Non-Metals at Horizontal Cylinders. Preprints of papers for Heat Transfer Symposium, Atlantic City (New Jersey), by Am. Inst. Chem. Eng., Dec. 5, 1951, pp. 55-76.
6. Lewis, J. A.: Boundary Layer in Compressible Fluid. Monograph V, Tech. Rep. No. F-TR-1179-ND(GDAM A-9-M V), Air Materiel Command (Dayton, Ohio), Feb. 1948. (Analysis Div., Intelligence Dept. Contract W33-038-ac-15004 (16351) with Brown Univ.)
7. Schlichting, Herman: *Grenzschicht-Theorie*. Verlag und Druck G. Braun, Karlsruhe, 1951, pp. 231-234.
8. Schmidt, Ernst und Beckmann, Wilhelm: Das Temperatur - und Geschwindigkeitsfeld vor einer Wärme abgebenden senkrechten Platte bei natürlicher Konvektion. *Tech. Mech. u. Thermodynamik*, Bd. 1, Nr. 10, Okt. 1930, S. 341-349; cont., Bd. 1, Nr. 11, Nov. 1930, S. 391-406.

9. Ostrach, Simon: A Boundary Layer Problem in the Theory of Free Convection. Doctoral Thesis, Brown Univ., Aug. 1950.
10. Eckert, E. R. G., and Jackson, Thomas W.: Analysis of Turbulent Free-Convection Boundary Layer on Flat Plate. NACA Rep. 1015, 1951. (Supersedes NACA TN 2207.)

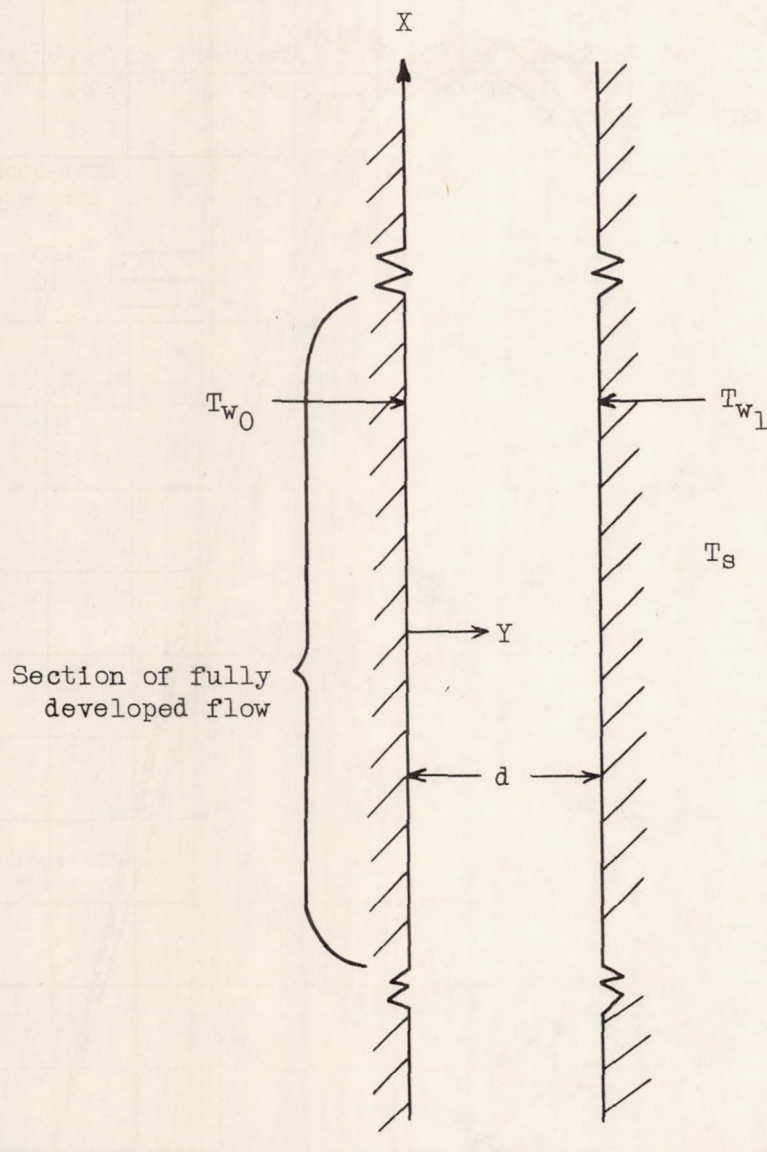
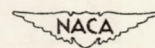


Figure 1. - Schematic sketch of simplified configuration.



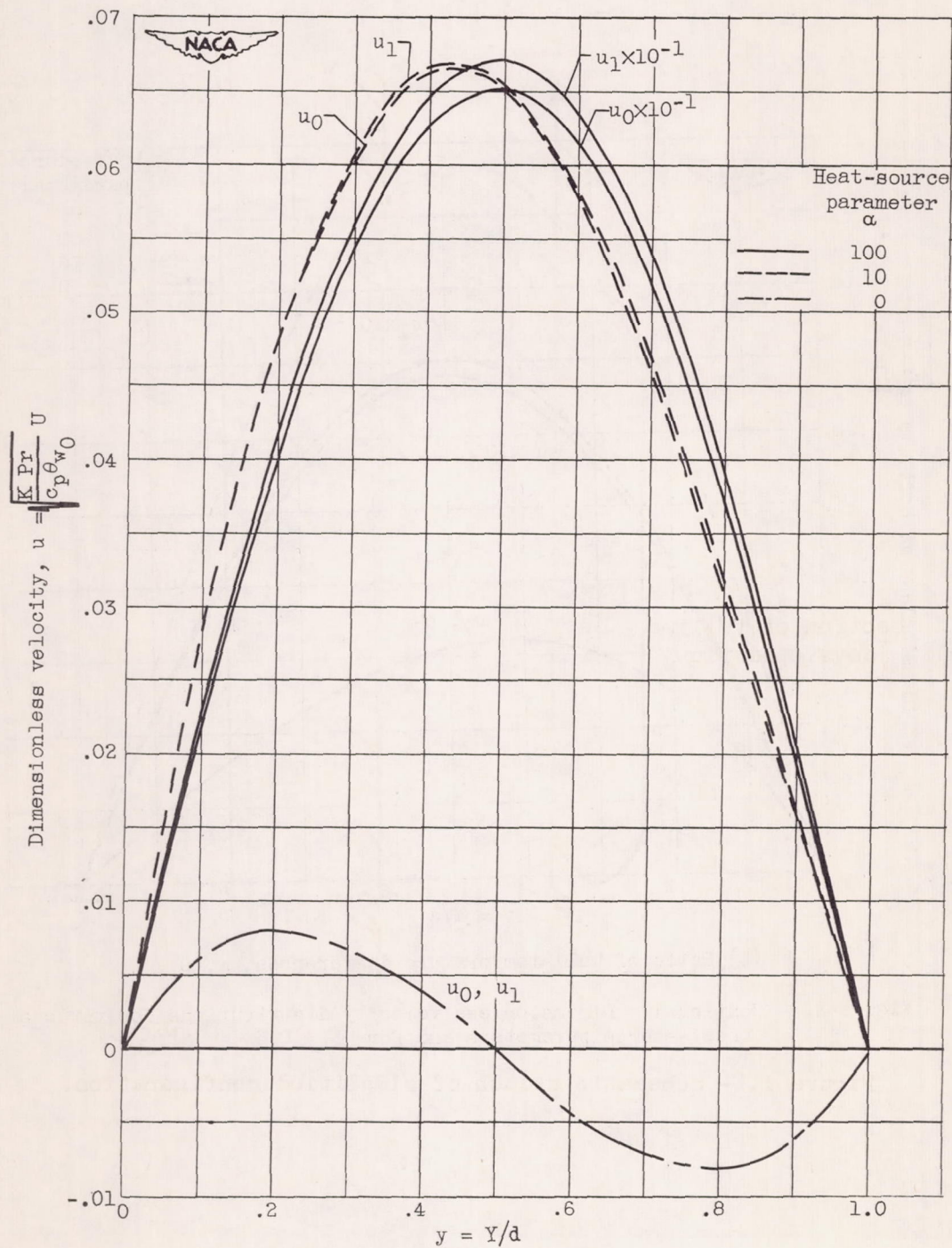
(a) Ratio of wall-temperature differences, m , -1.

Figure 2. - Dimensionless velocity distributions for various heat-source parameters and for $K = 0.5$.

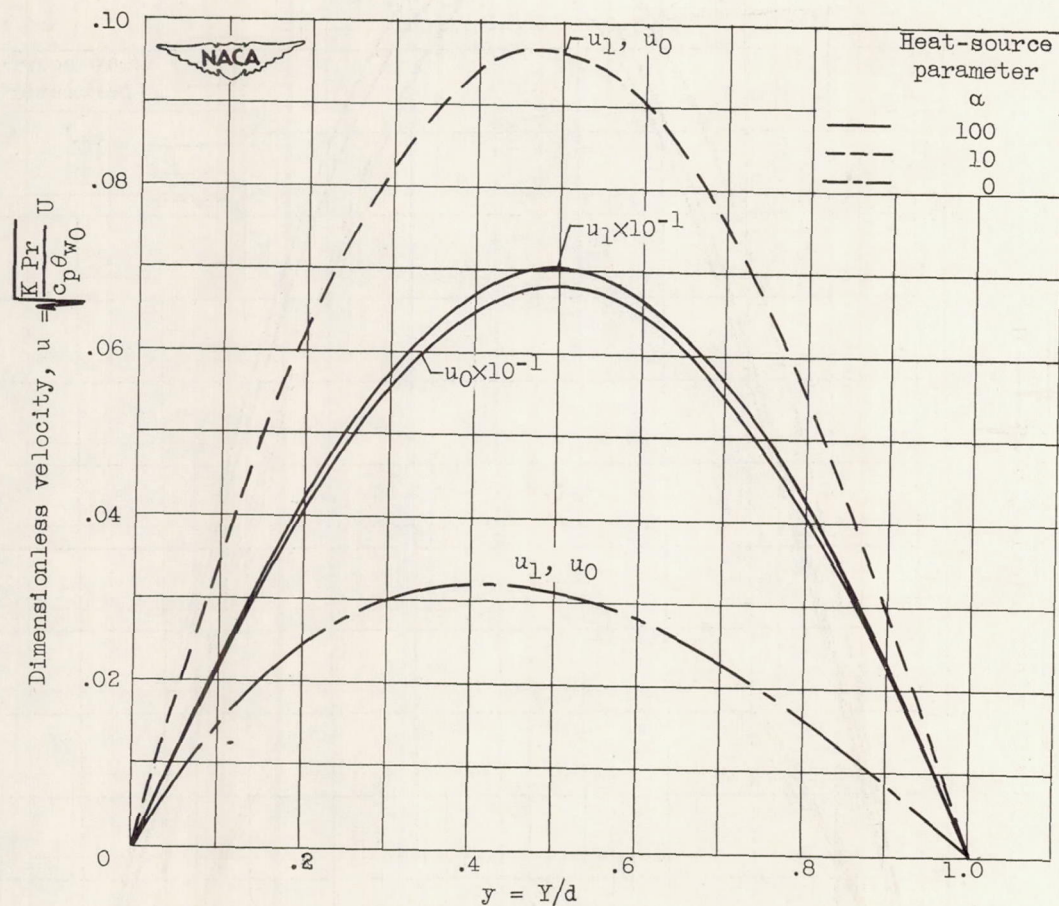
(b) Ratio of wall-temperature differences, m , 0.

Figure 2. - Continued. Dimensionless velocity distributions for various heat-source parameters and for $K = 0.5$.

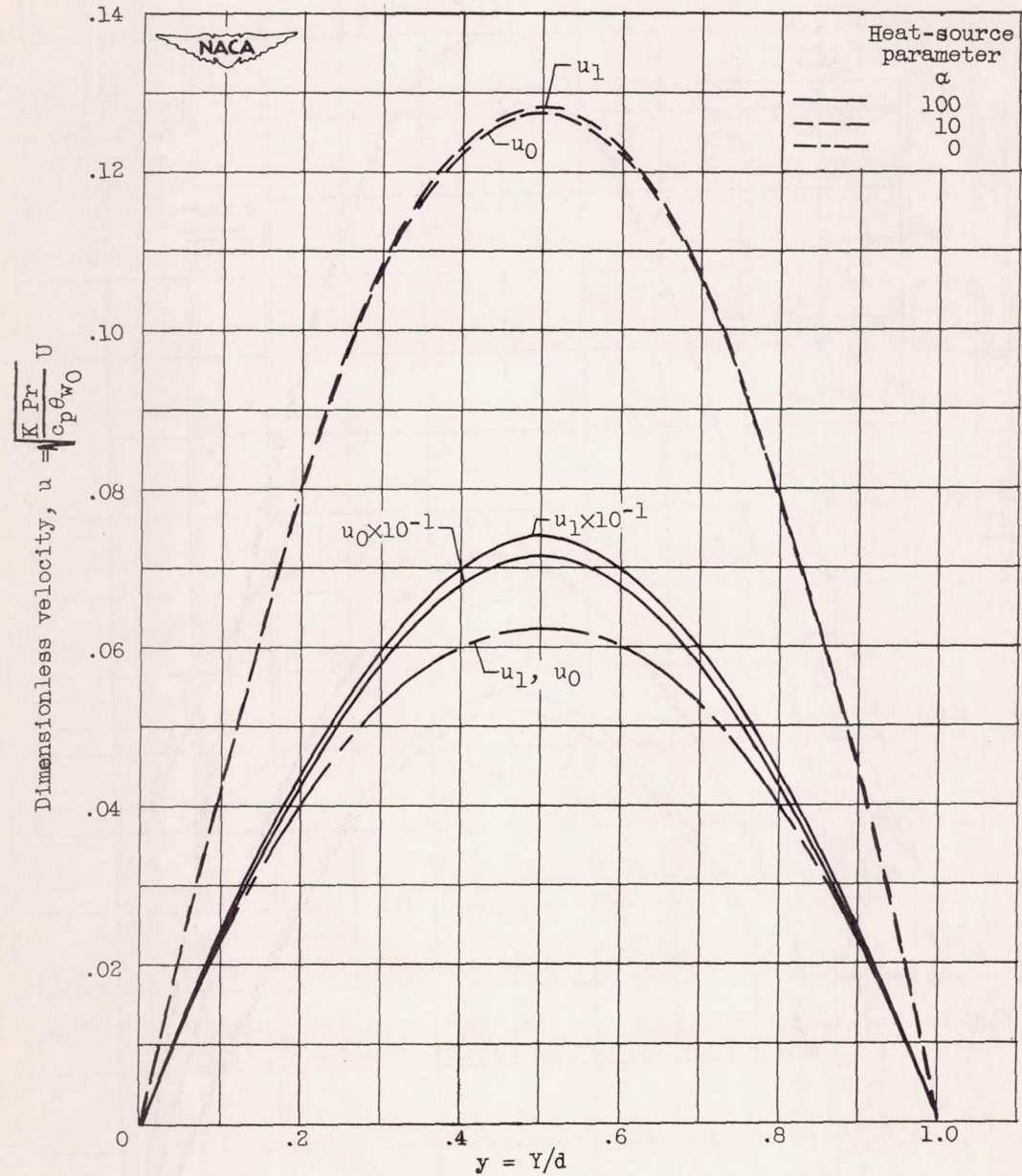
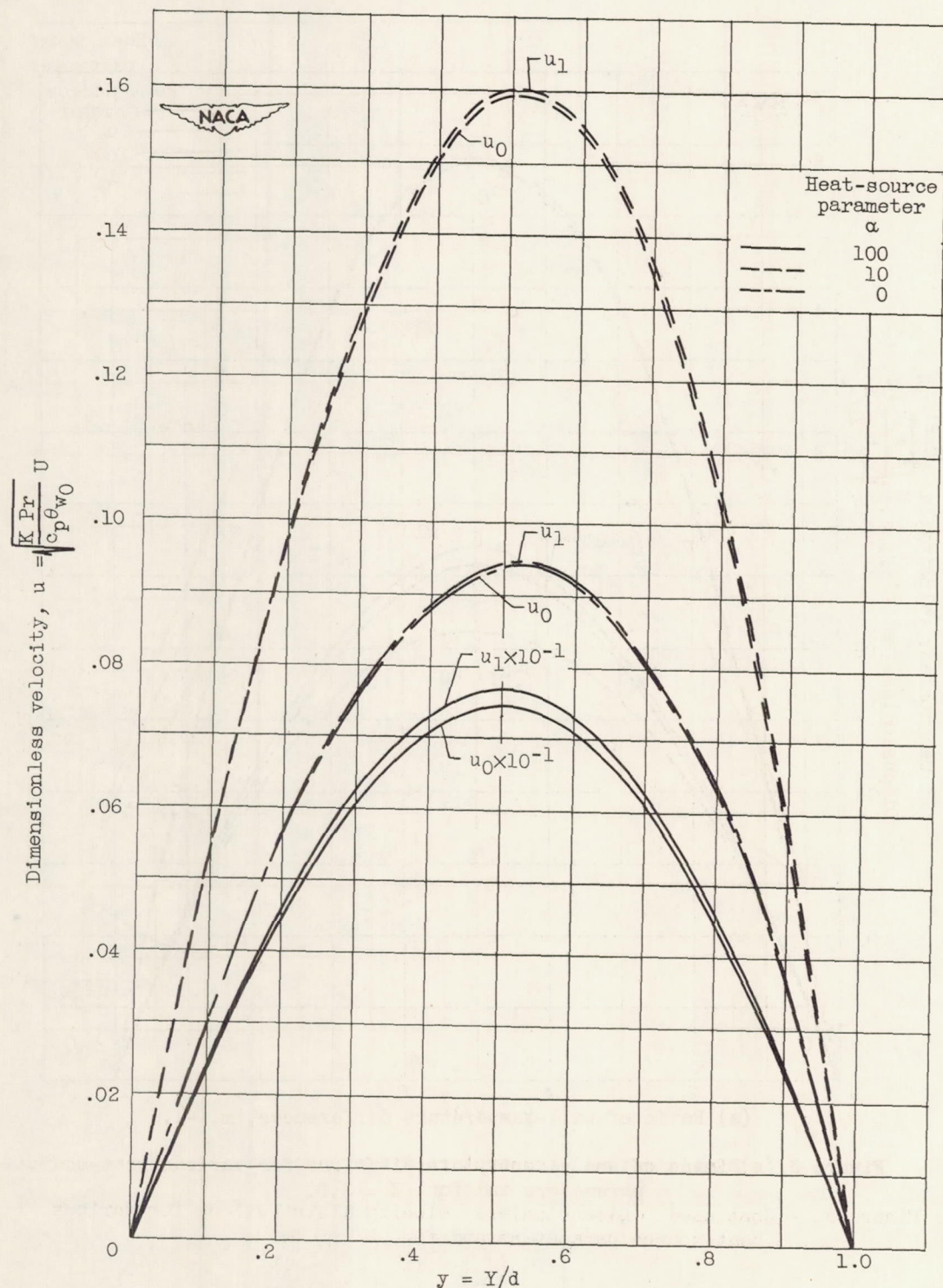
(c) Ratio of wall-temperature differences, m, l .

Figure 2. - Continued. Dimensionless velocity distributions for various heat-source parameters and for $K = 0.5$.



(d) Ratio of wall-temperature differences, m , 2.

Figure 2. - Concluded. Dimensionless velocity distributions for various heat-source parameters and for $K = 0.5$.

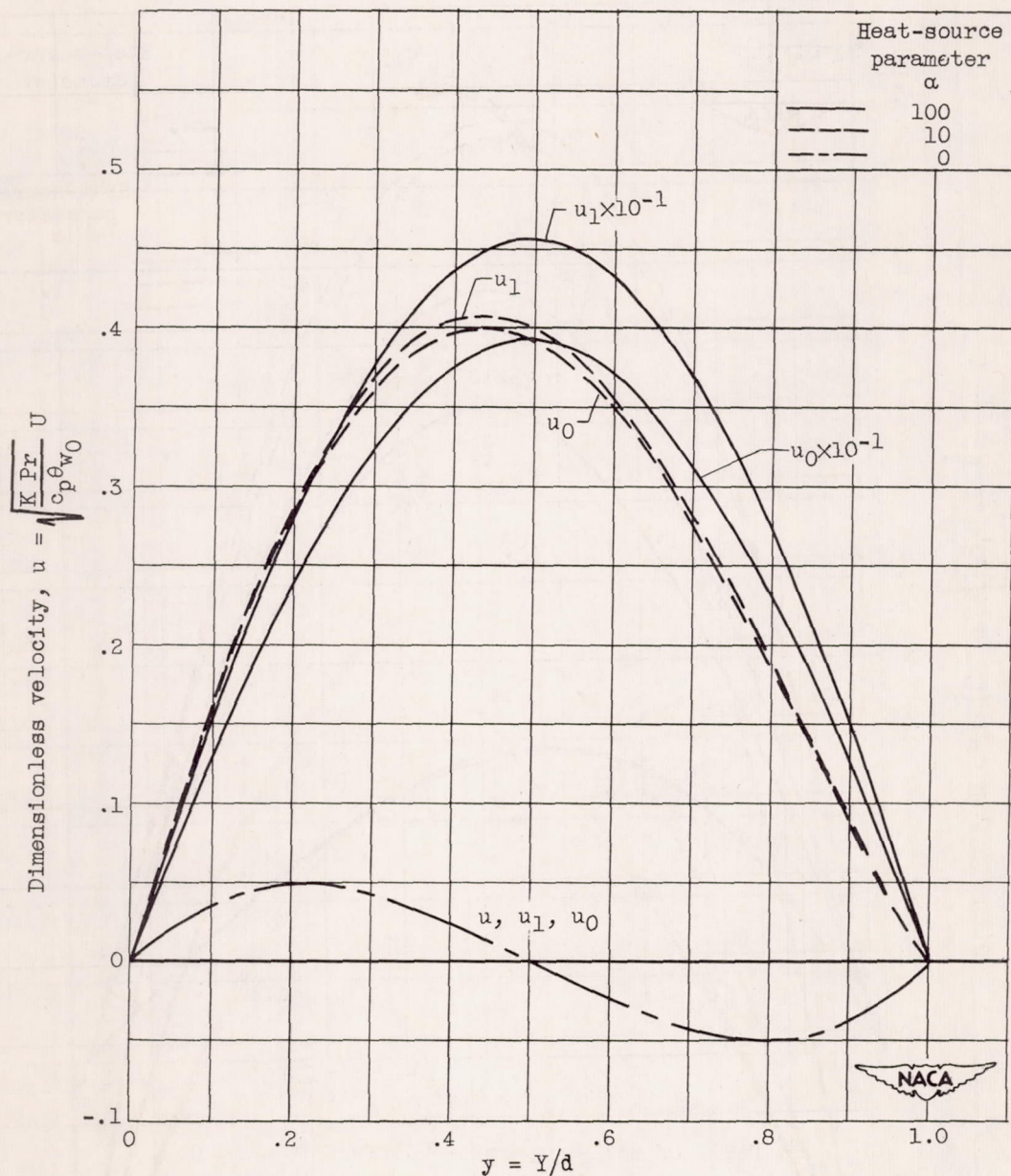
(a) Ratio of wall-temperature differences, $m, -1$.

Figure 3. - Dimensionless velocity distributions for various heat-source parameters and for $K = 3.0$.

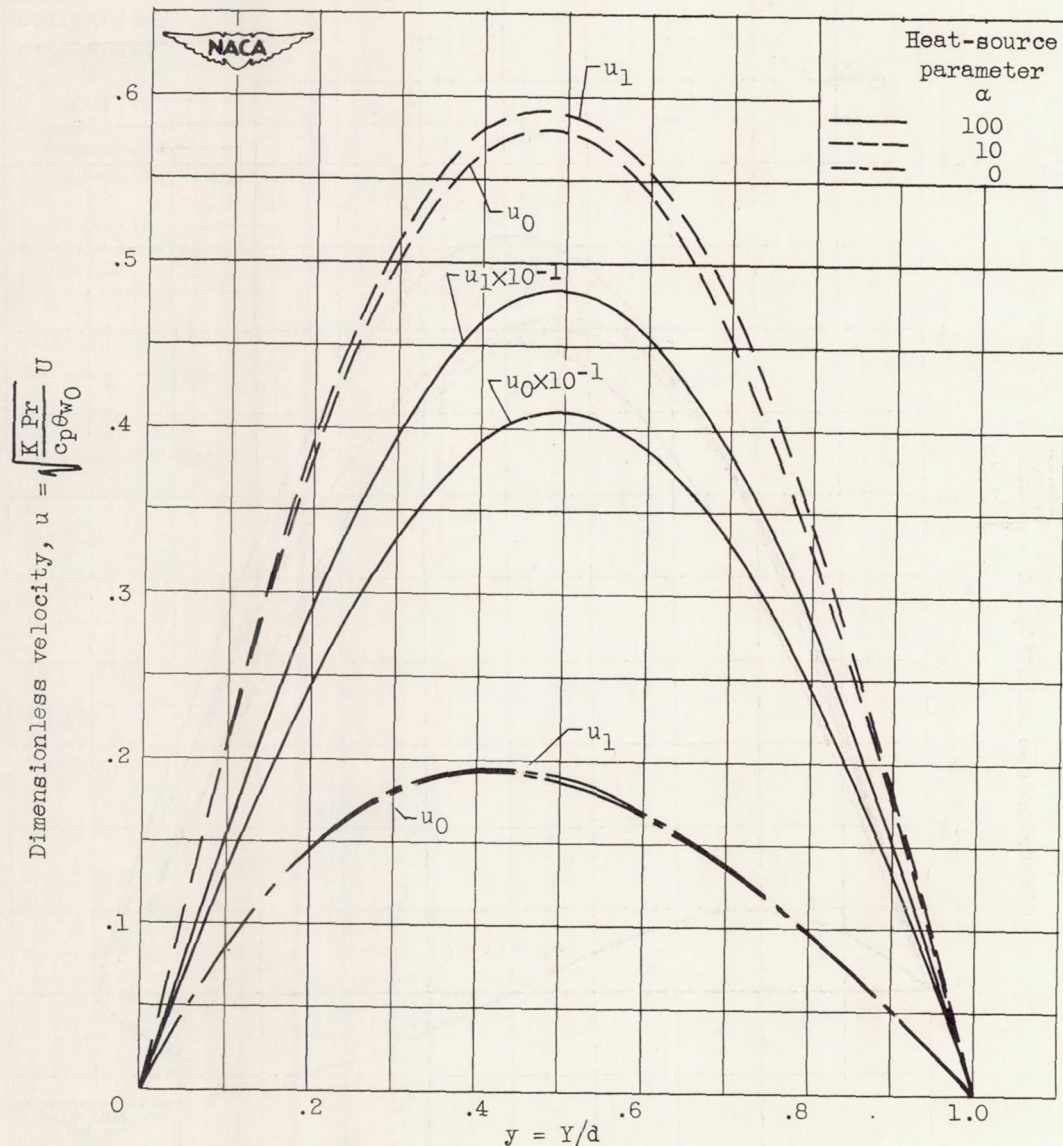
(b) Ratio of wall-temperature differences, m , 0.

Figure 3. - Continued. Dimensionless velocity distributions for various heat-source parameters and for $K = 3.0$.

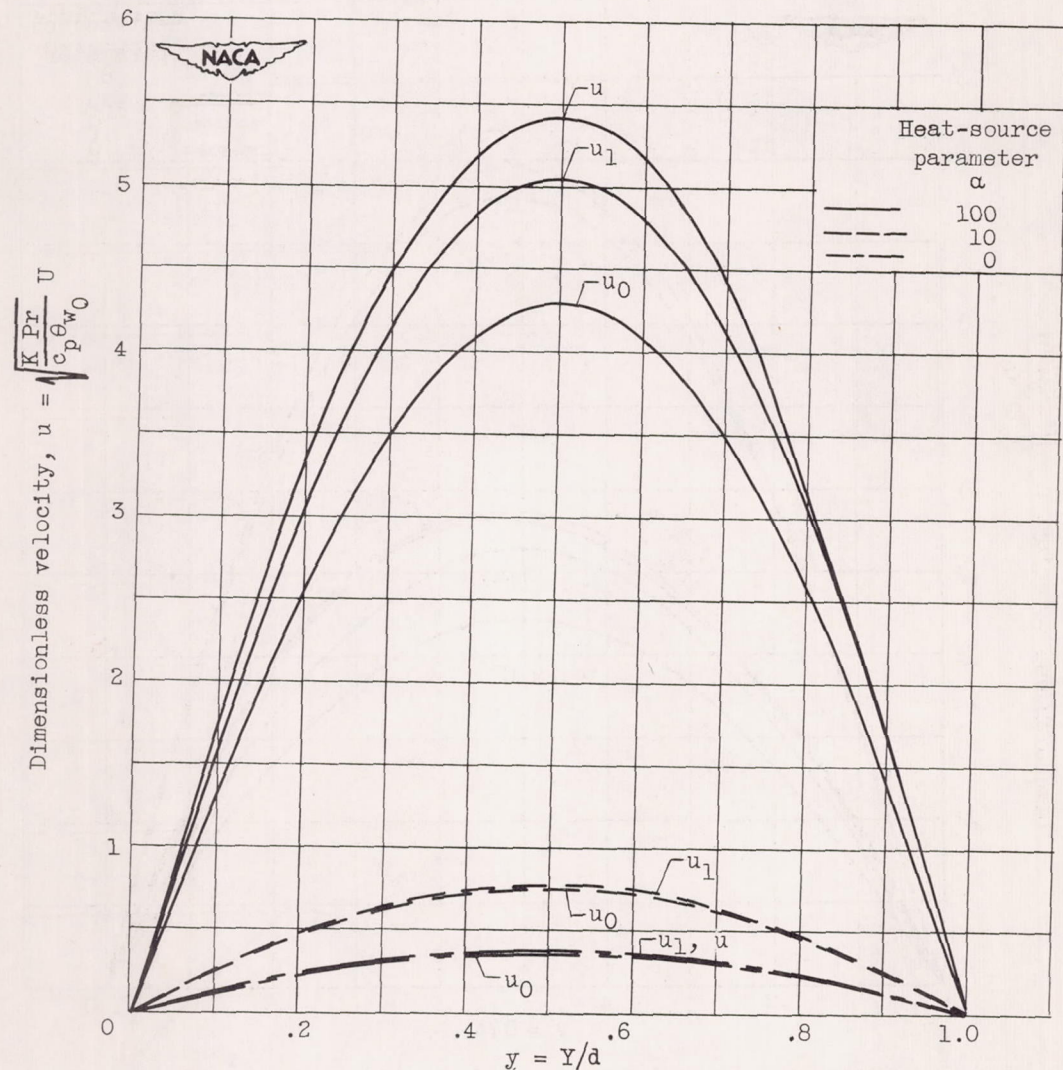
(c) Ratio of wall-temperature difference, m , 1.

Figure 3. - Continued. Dimensionless velocity distributions for various heat-source parameters and for $K = 3.0$.

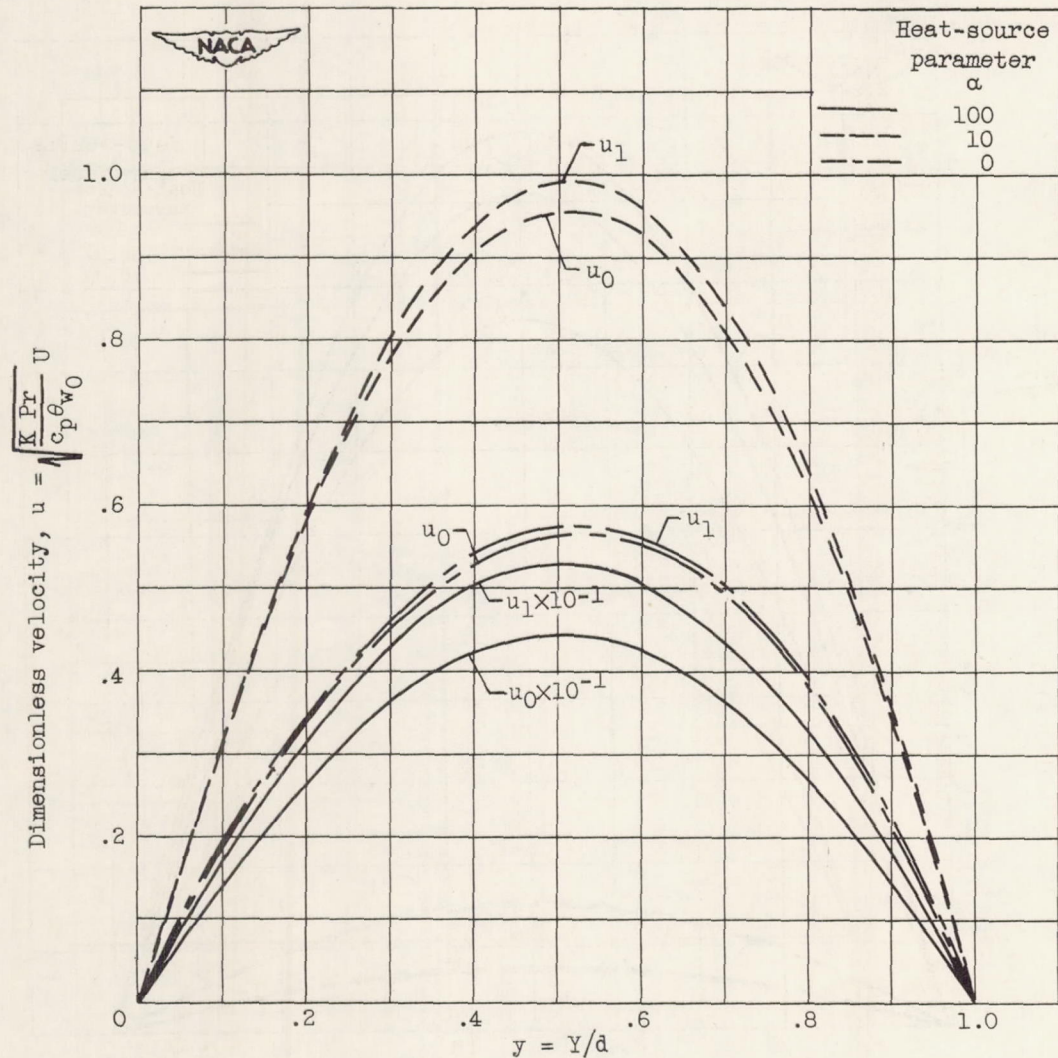
(d) Ratio of wall-temperature differences, m , 2.

Figure 3. - Concluded. Dimensionless velocity distributions for various heat-source parameters and for $K = 3.0$.

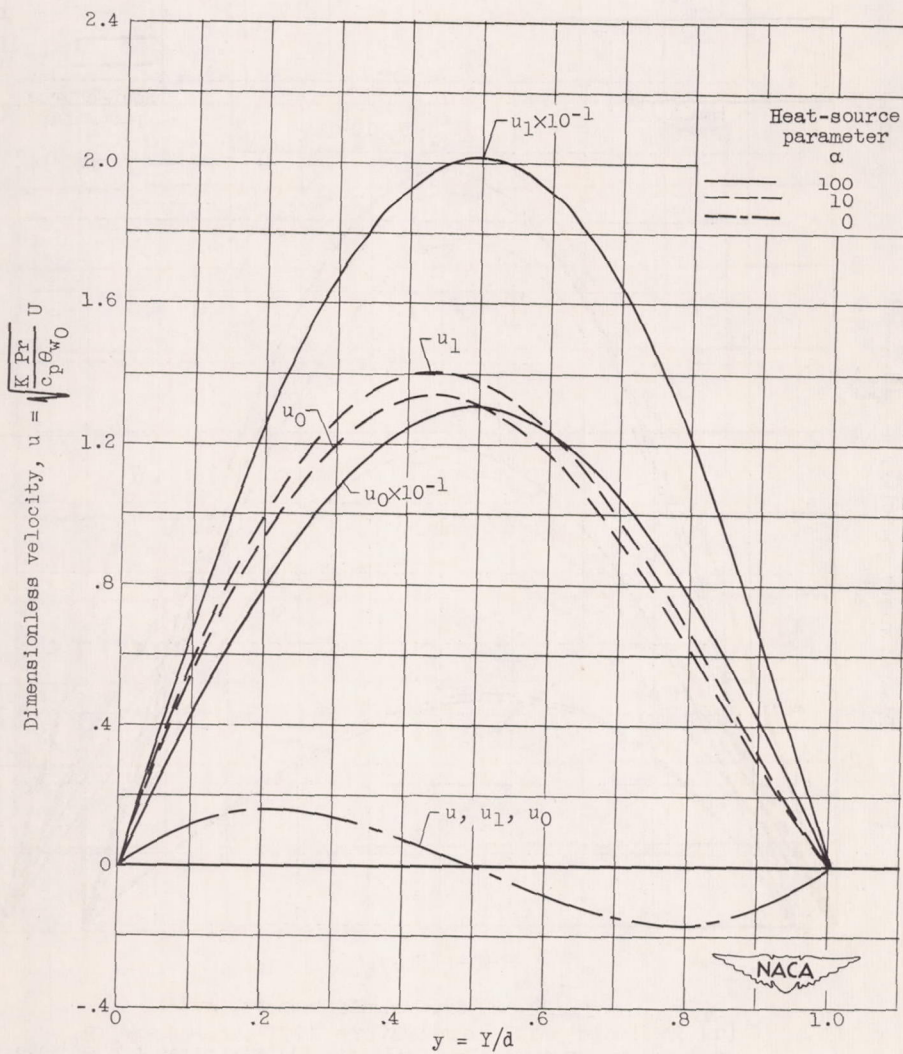
(a) Ratio of wall-temperature differences, $m, -1$.

Figure 4. - Dimensionless velocity distributions for various heat-source parameters and for $K = 10.0$.

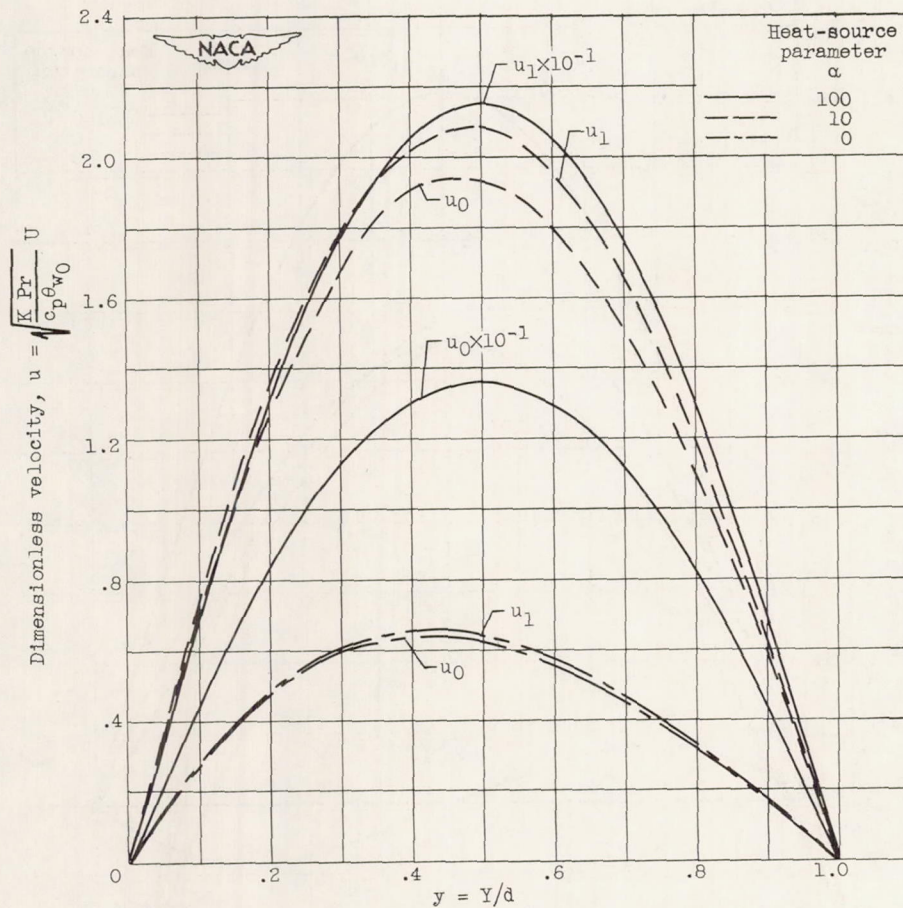
(b) Ratio of wall-temperature differences, m , 0.

Figure 4. - Continued. Dimensionless velocity distributions for various heat-source parameters and for $K = 10.0$.

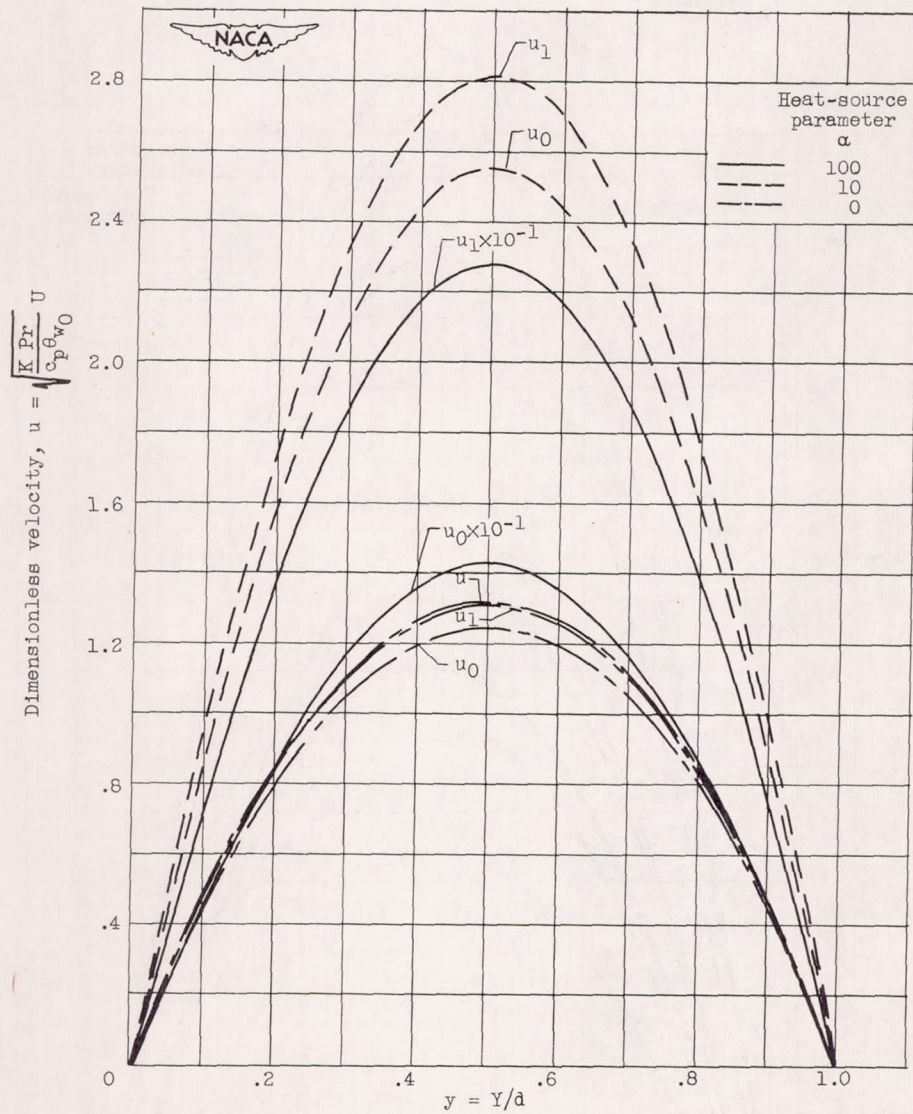
(c) Ratio of wall-temperature differences, m , 1.

Figure 4. - Continued. Dimensionless velocity distributions for various heat-source parameters and for $K = 10.0$.

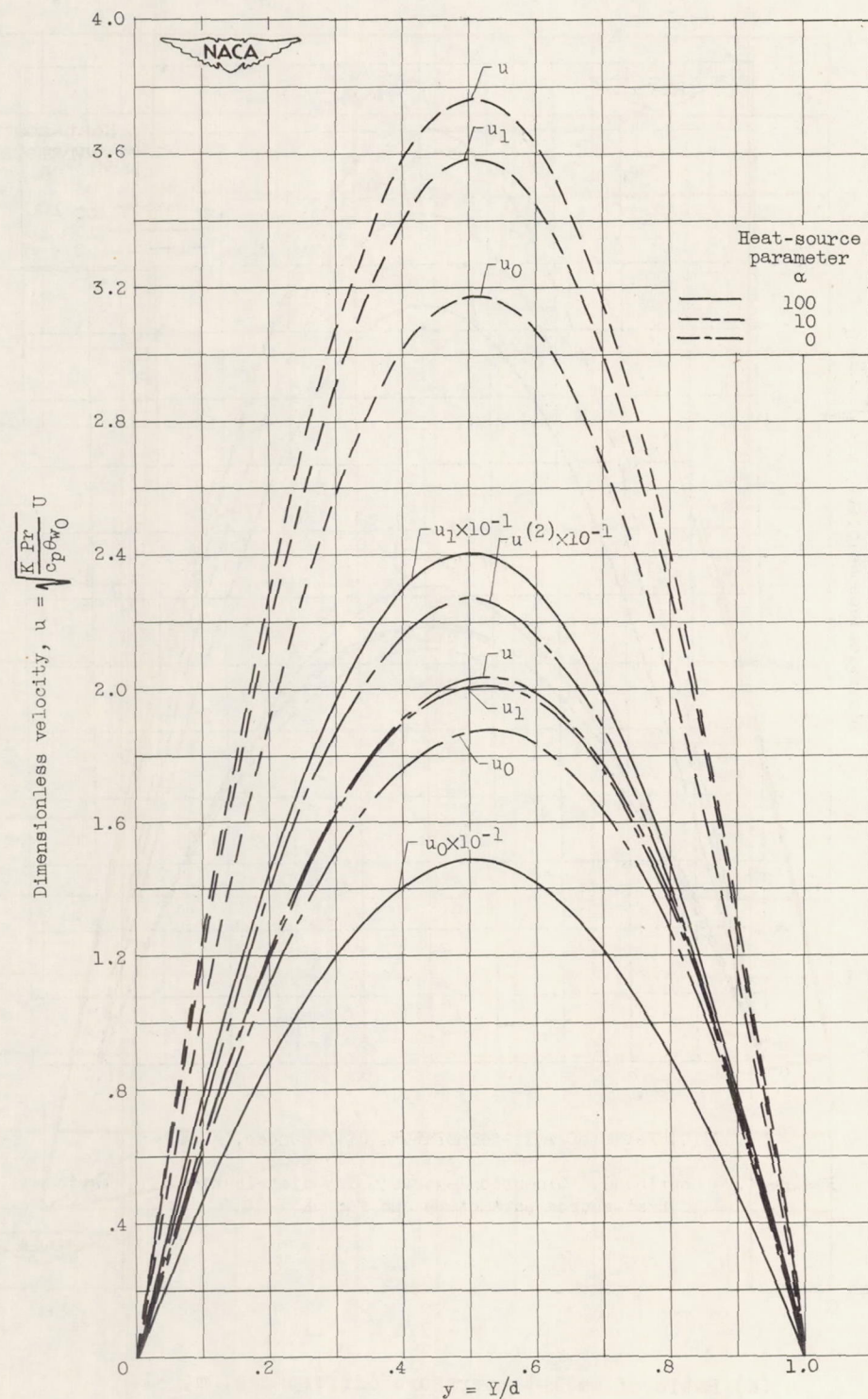
(a) Ratio of wall-temperature differences, m , 2.

Figure 4. - Concluded. Dimensionless velocity distributions for various heat-source parameters for $K = 10.0$.

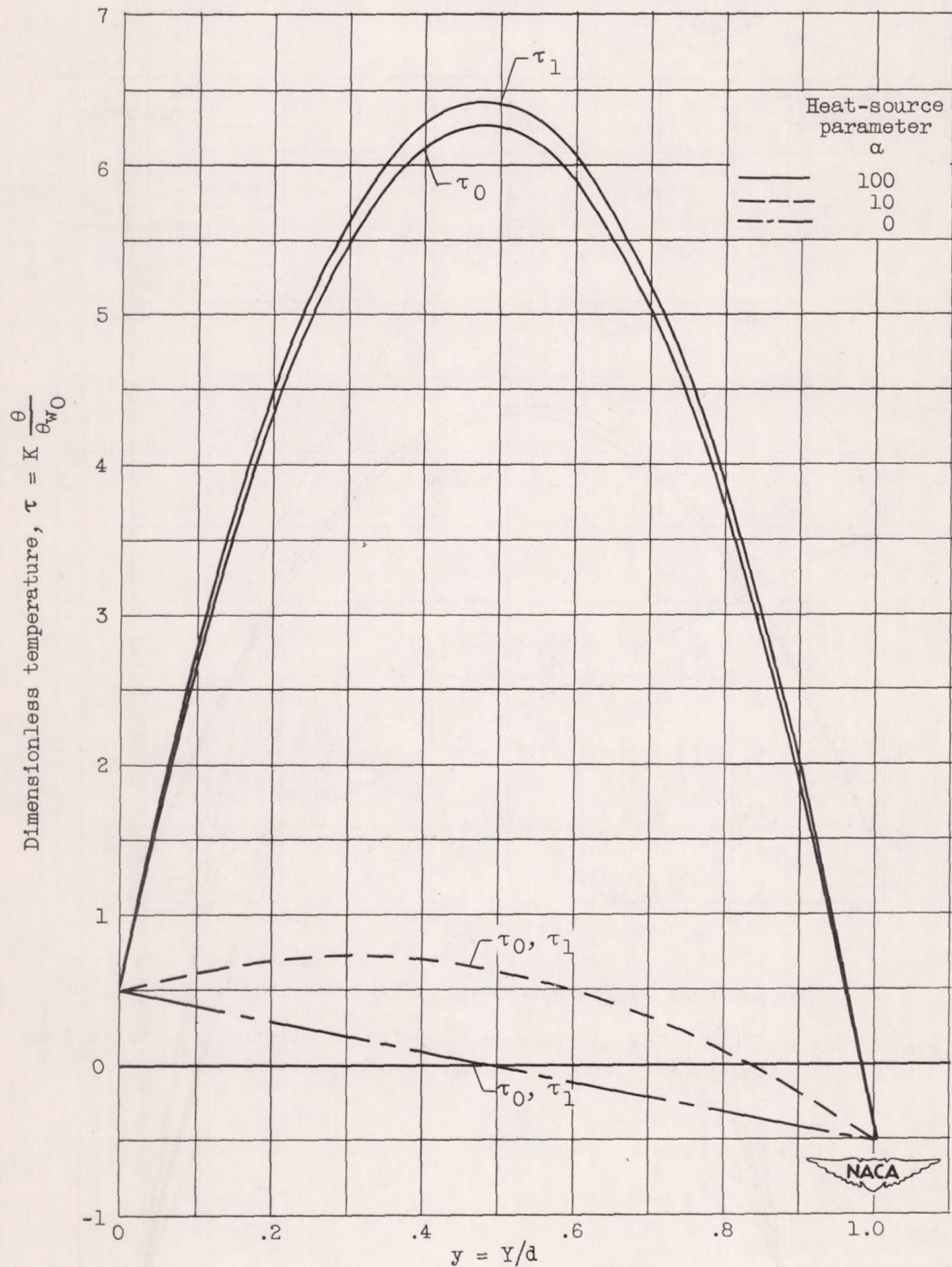
(a) Ratio of wall-temperature differences, m , -1.

Figure 5. - Dimensionless temperature distributions for various heat-source parameters and for $K = 0.5$.

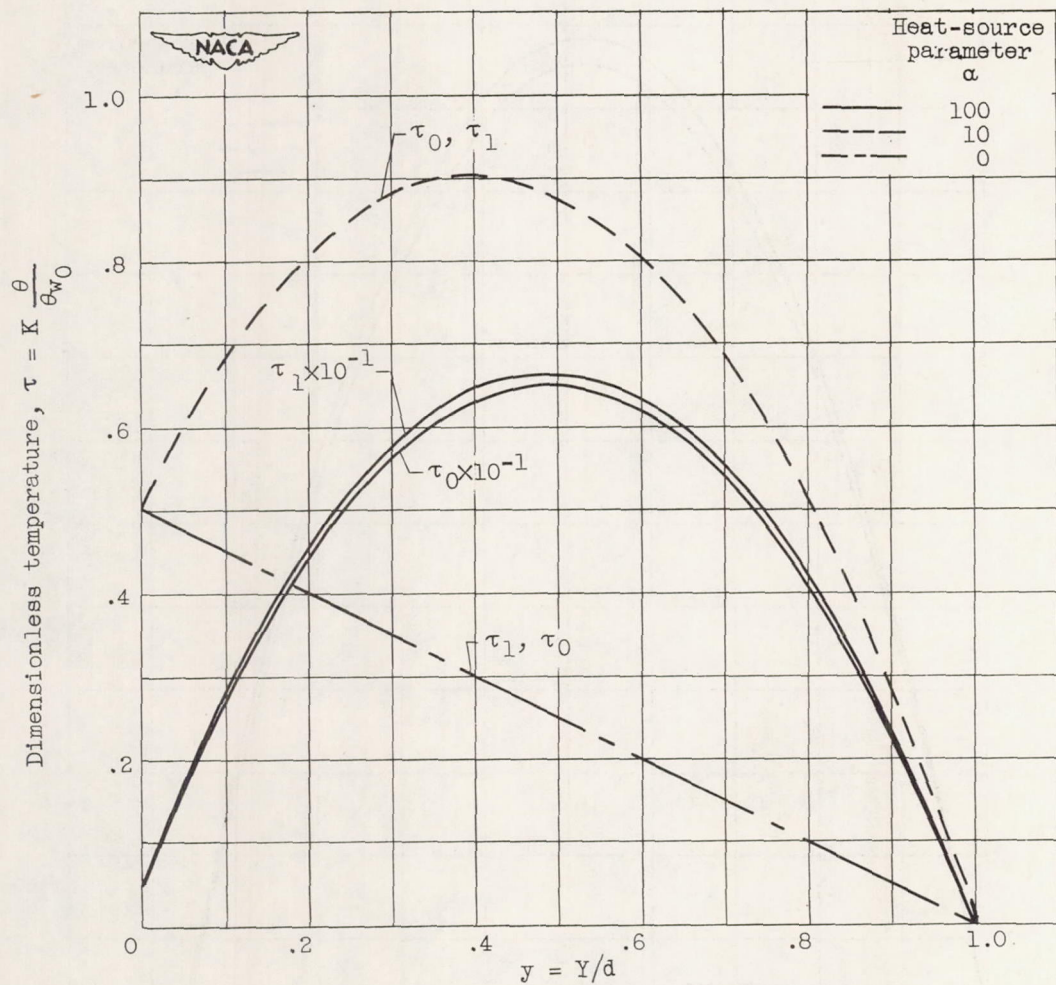
(b) Ratio of wall-temperature differences, m , 0.

Figure 5. - Continued. Dimensionless temperature distributions for various heat-source parameters and for $K = 0.5$.

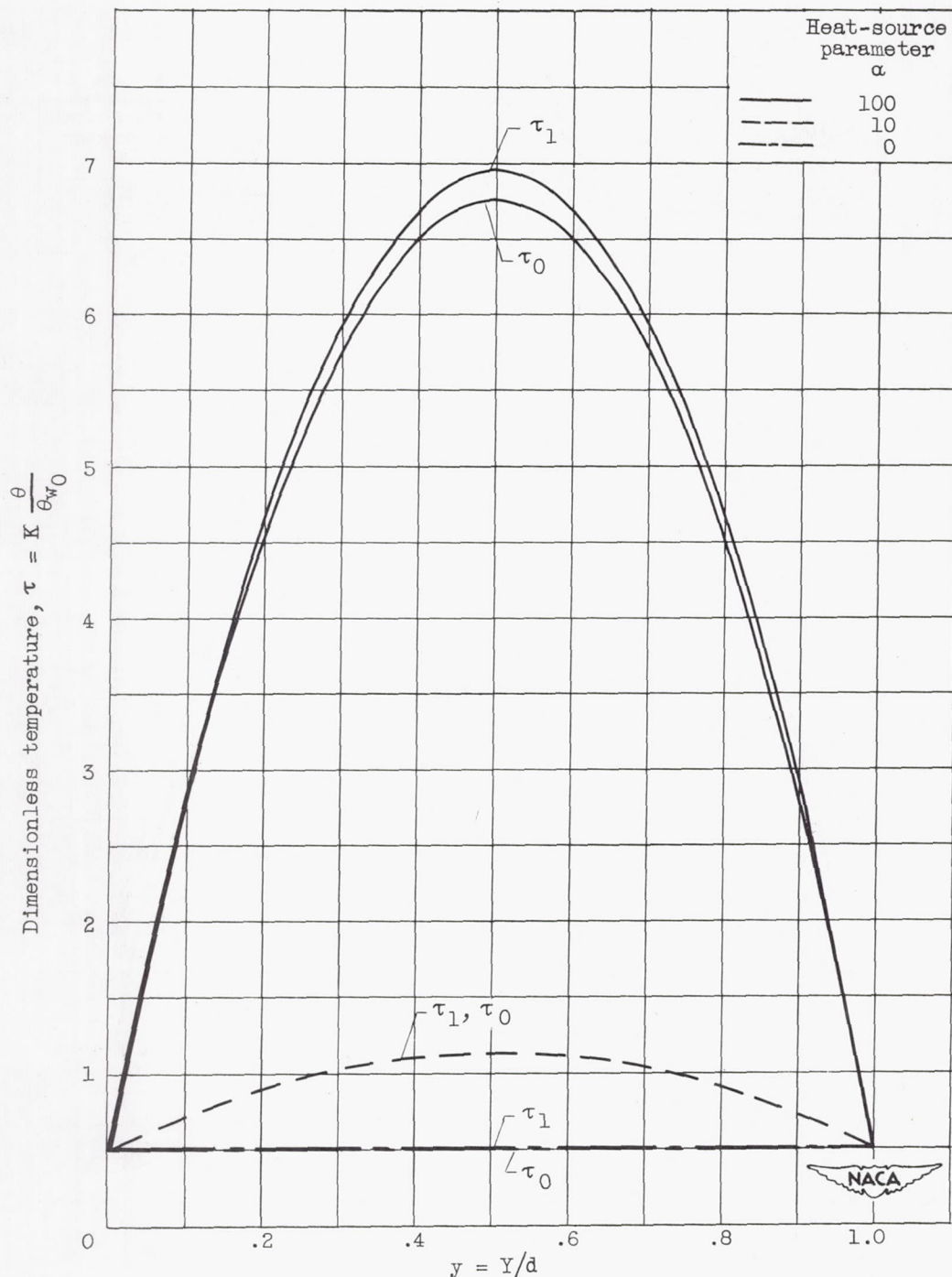
(c) Ratio of wall-temperature differences, m , 1.

Figure 5. - Continued. Dimensionless temperature distributions for various heat-source parameters and for $K = 0.5$.

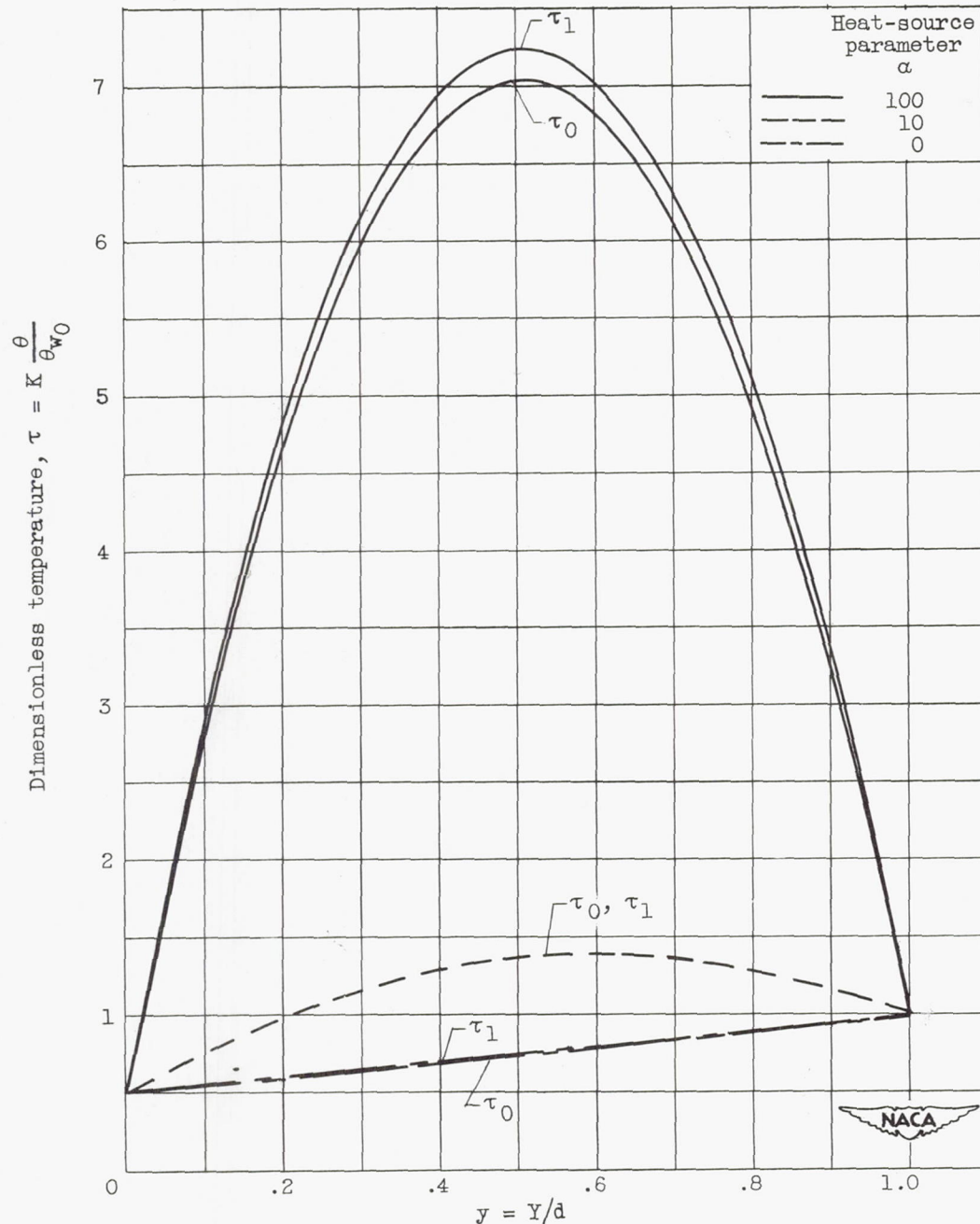
(a) Ratio of wall-temperature differences, m , 2.

Figure 5. - Concluded. Dimensionless temperature distributions for various heat-source parameters and for $K = 0.5$.

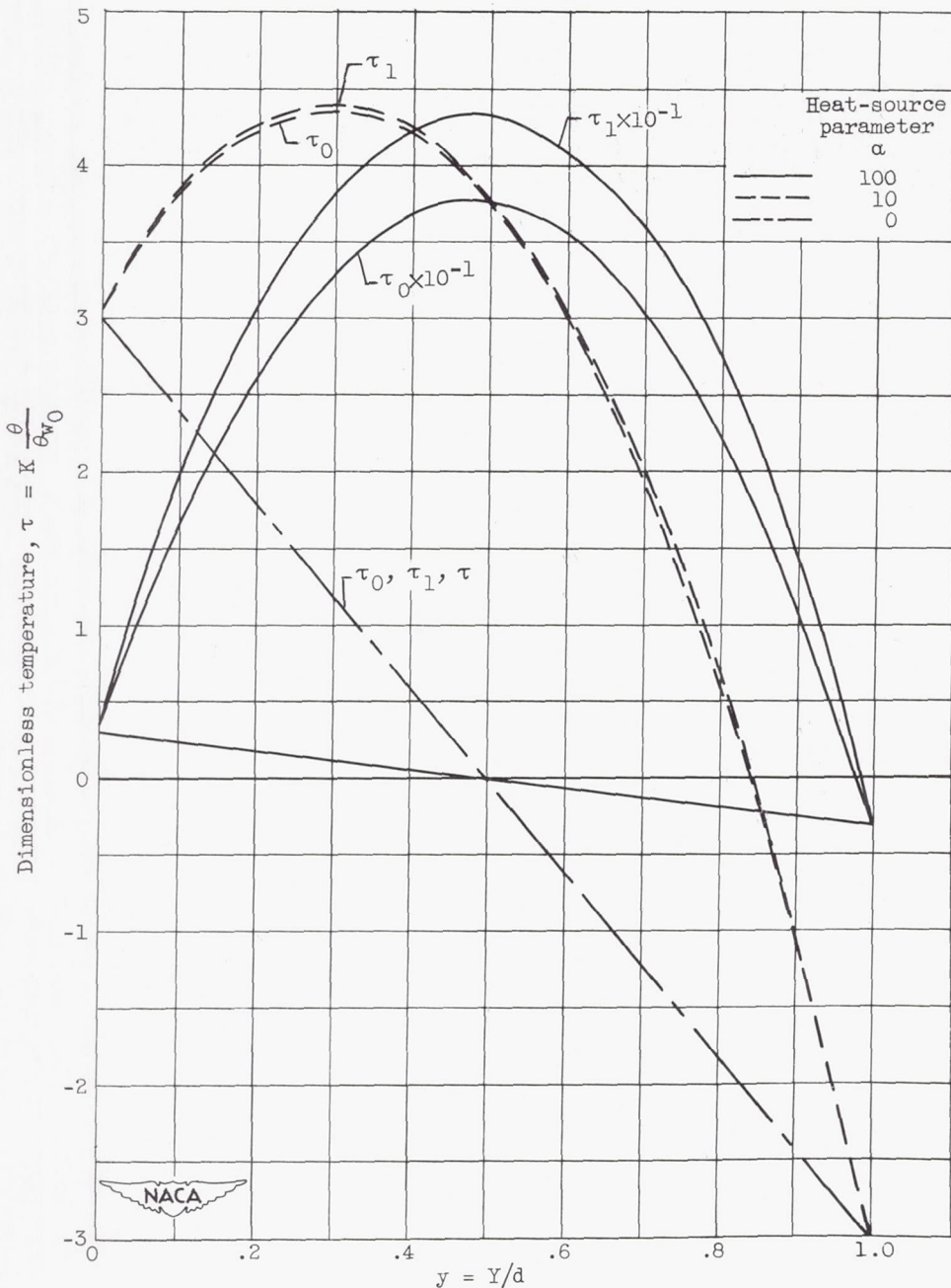
(a) Ratio of wall-temperature differences, m , -1 .

Figure 6. - Dimensionless temperature distributions for various heat-source parameters and for $K = 3.0$.

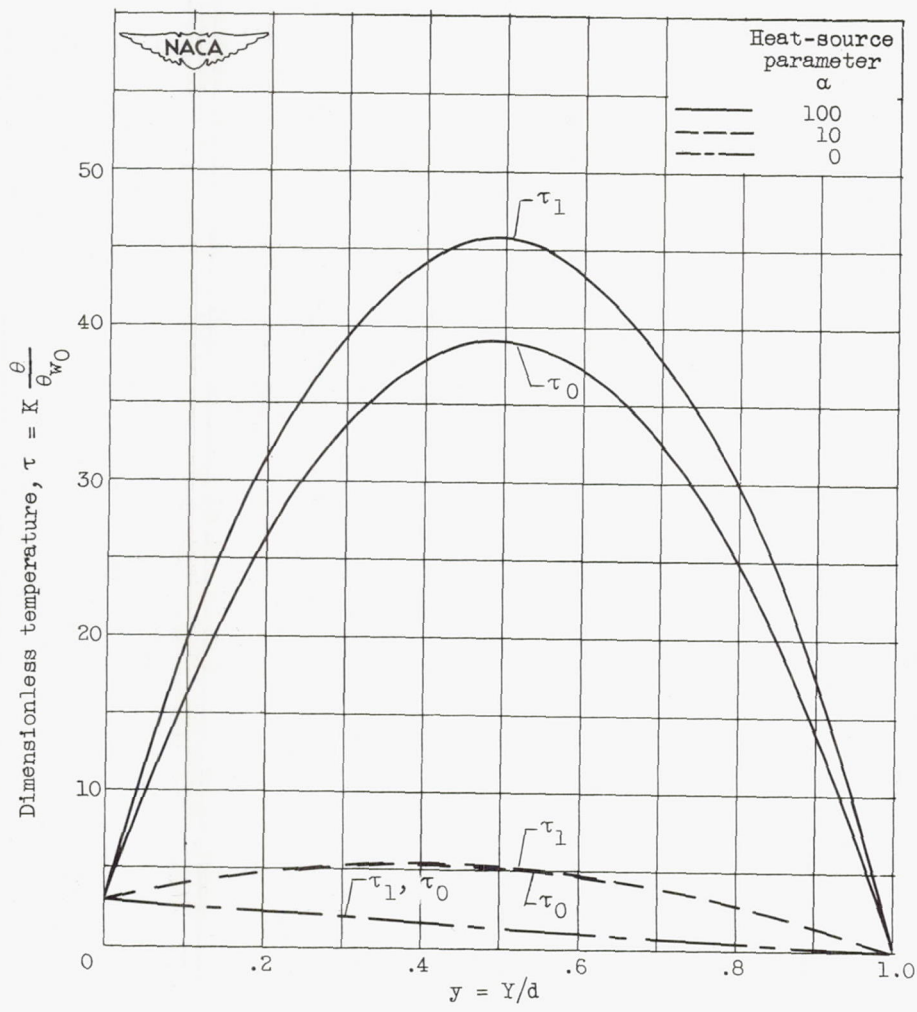
(b) Ratio of wall-temperature differences, $m, 0.$

Figure 6. - Continued. Dimensionless temperature distributions for various heat-source parameters and for $K = 3.0$.

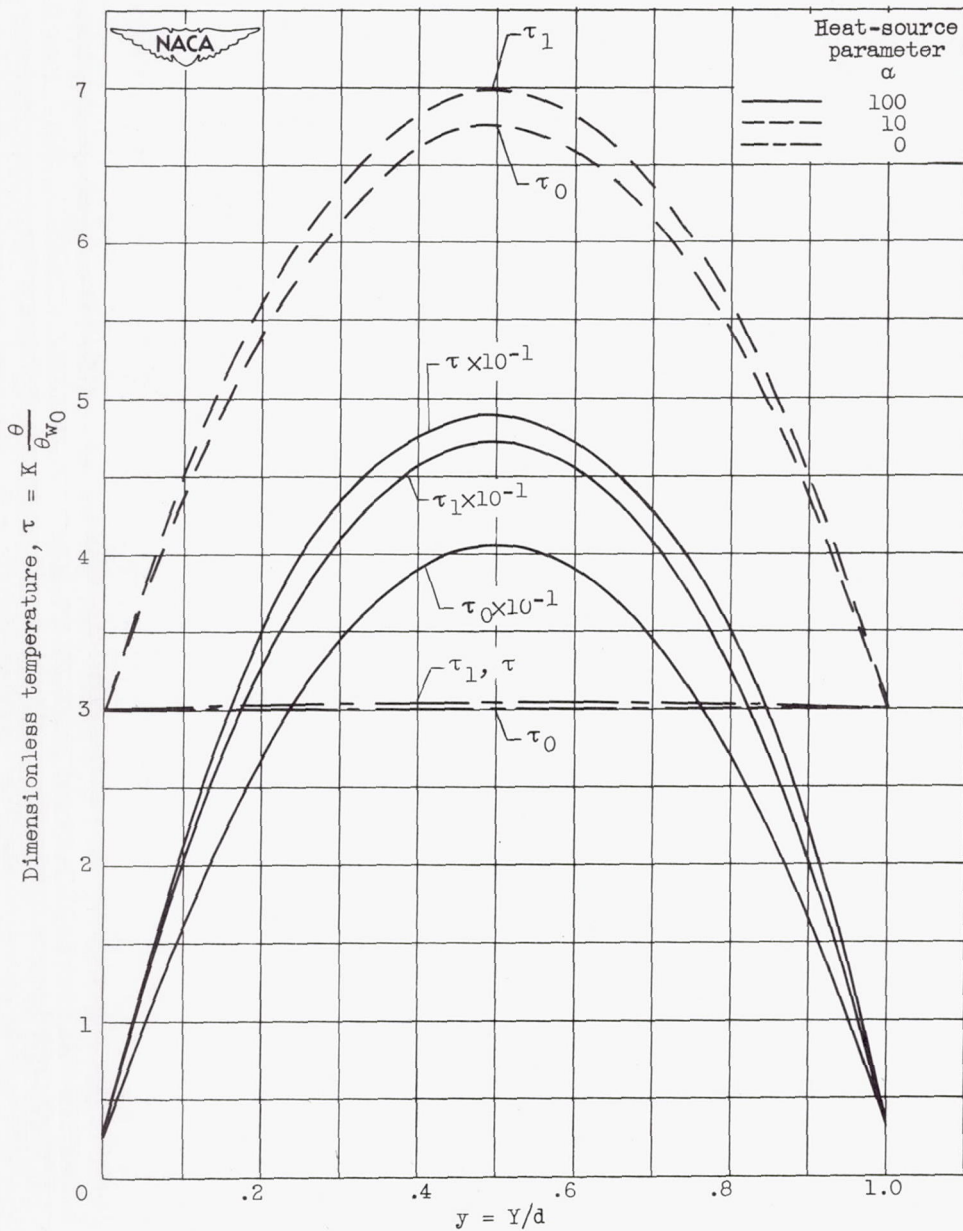
(c) Ratio of wall-temperature differences, m , 1.

Figure 6. - Continued. Dimensionless temperature distributions for various heat-source parameters and for $K = 3.0$.

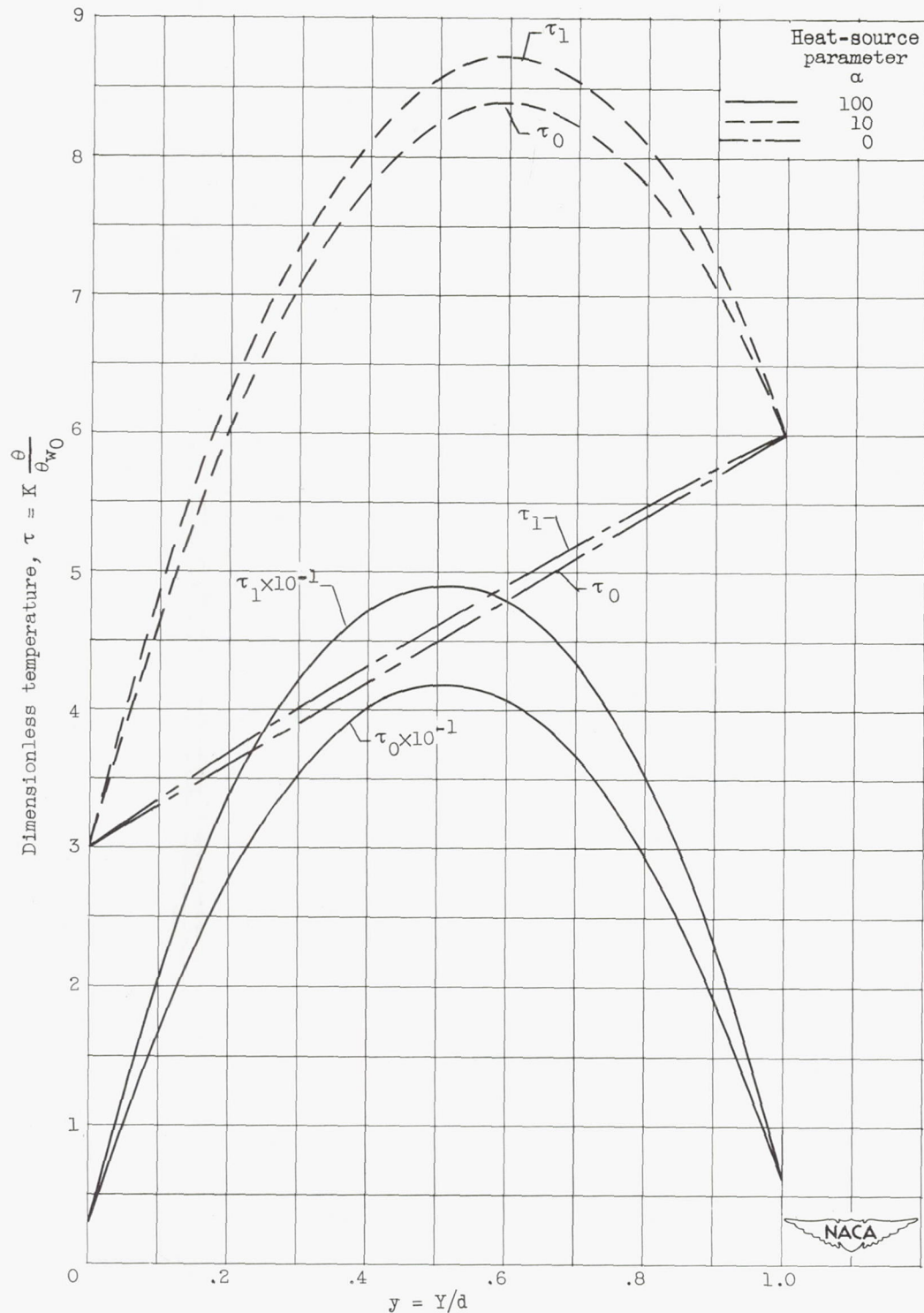
(d) Ratio of wall-temperature differences, m , 2.

Figure 6. - Concluded. Dimensionless temperature distributions for various heat-source parameters and for $K = 3.0$.

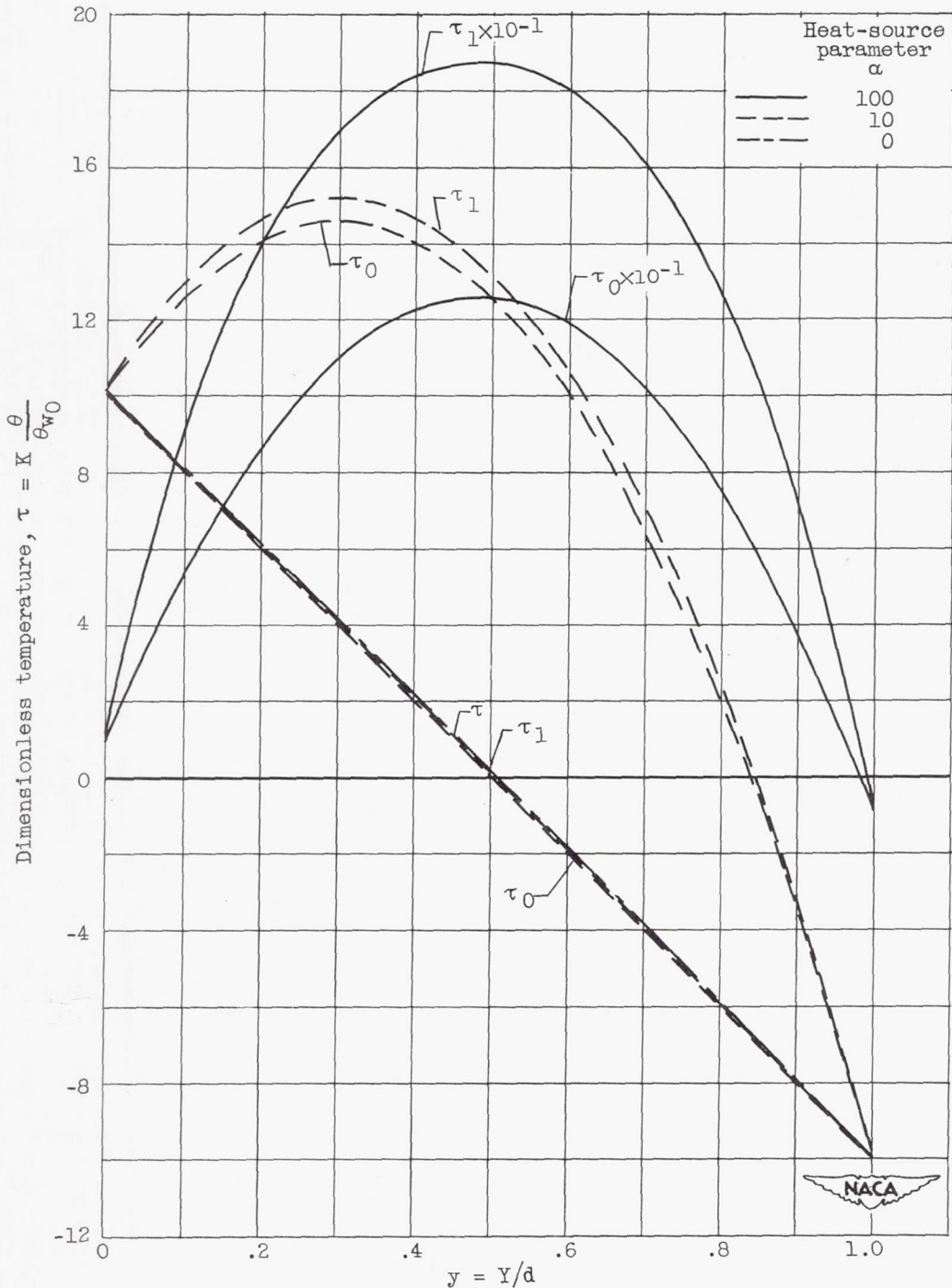
(a) Ratio of wall-temperature differences, m , -1.

Figure 7. - Dimensionless temperature distributions for various heat-source parameters and for $K = 10.0$.

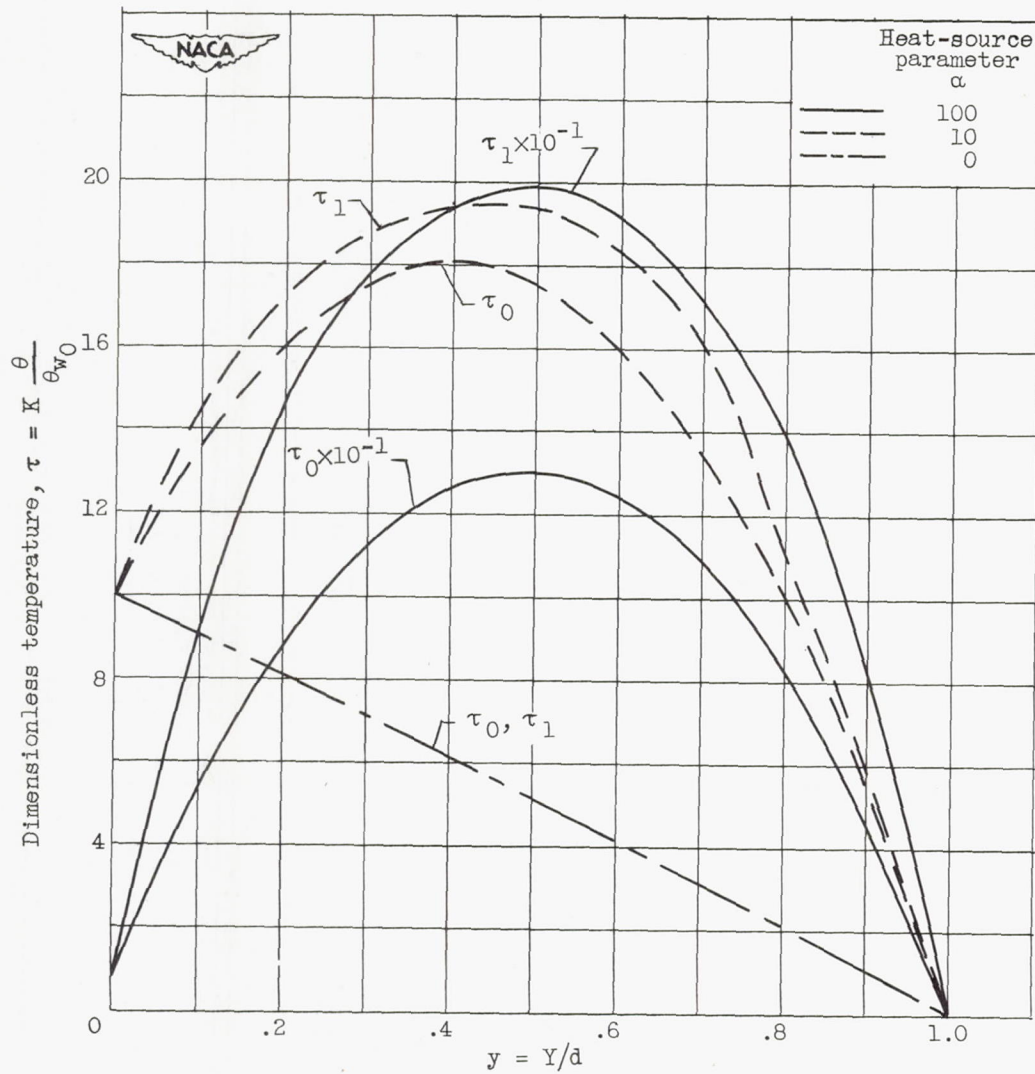
(b) Ratio of wall-temperature differences, $m, 0$.

Figure 7. - Continued. Dimensionless temperature distributions for various heat-source parameters and for $K = 10.0$.

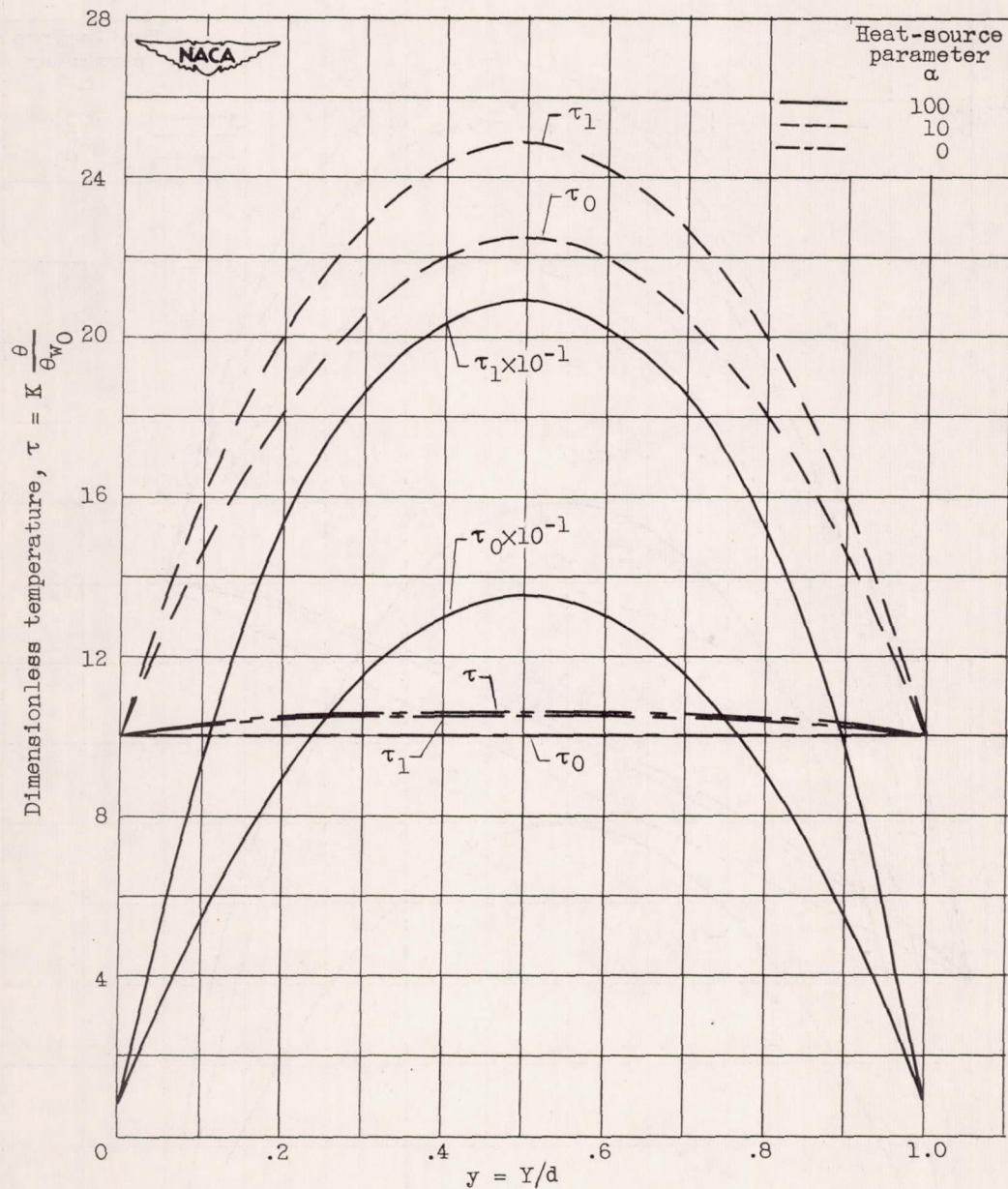
(c) Ratio of wall-temperature differences, m , 1.

Figure 7. - Continued. Dimensionless temperature distributions for various heat-source parameters and for $K = 10.0$.

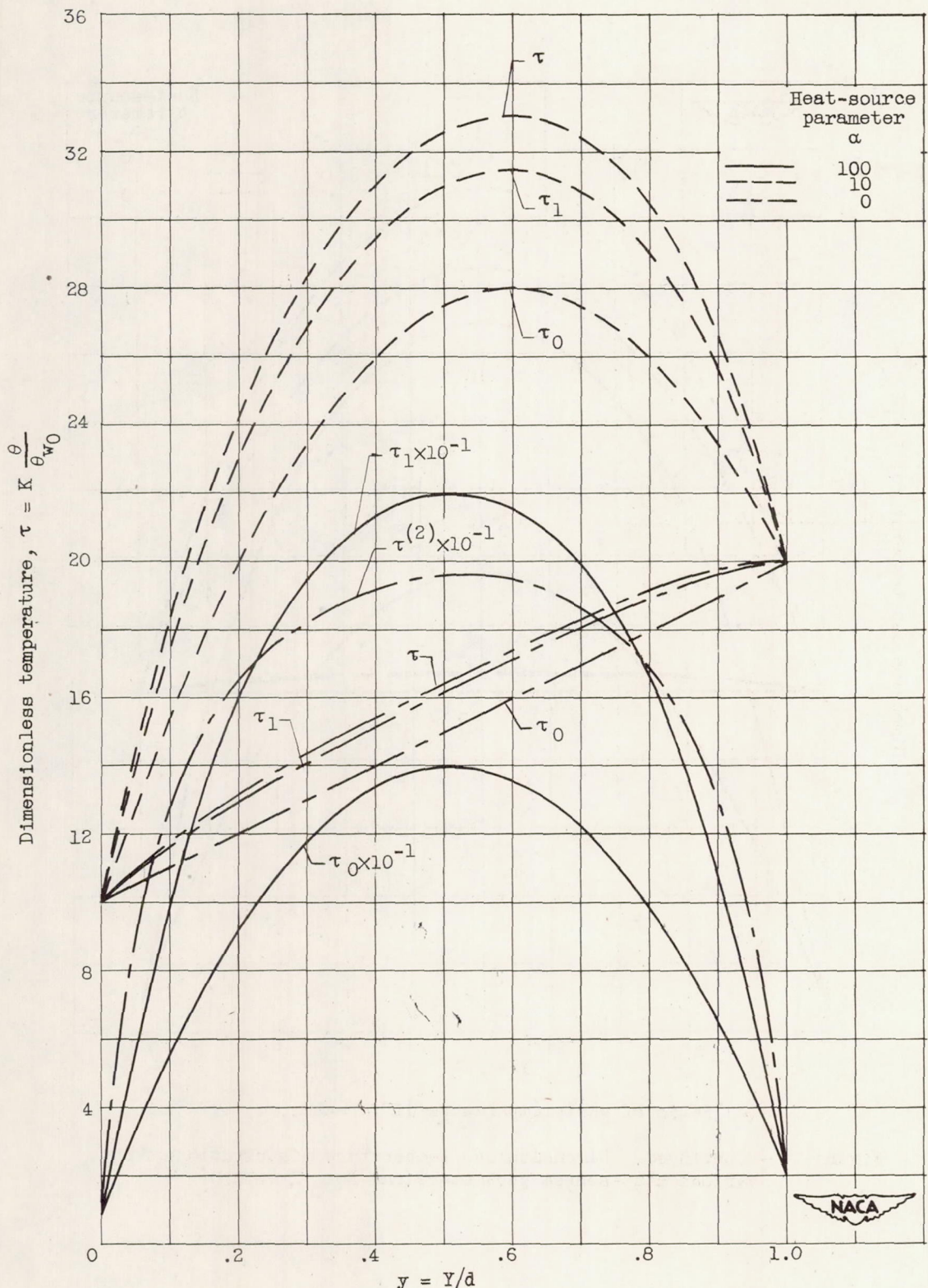
(d) Ratio of wall-temperature differences, m , 2.

Figure 7. - Concluded. Dimensionless temperature distributions for various heat-source parameters and for $K = 10.0$.

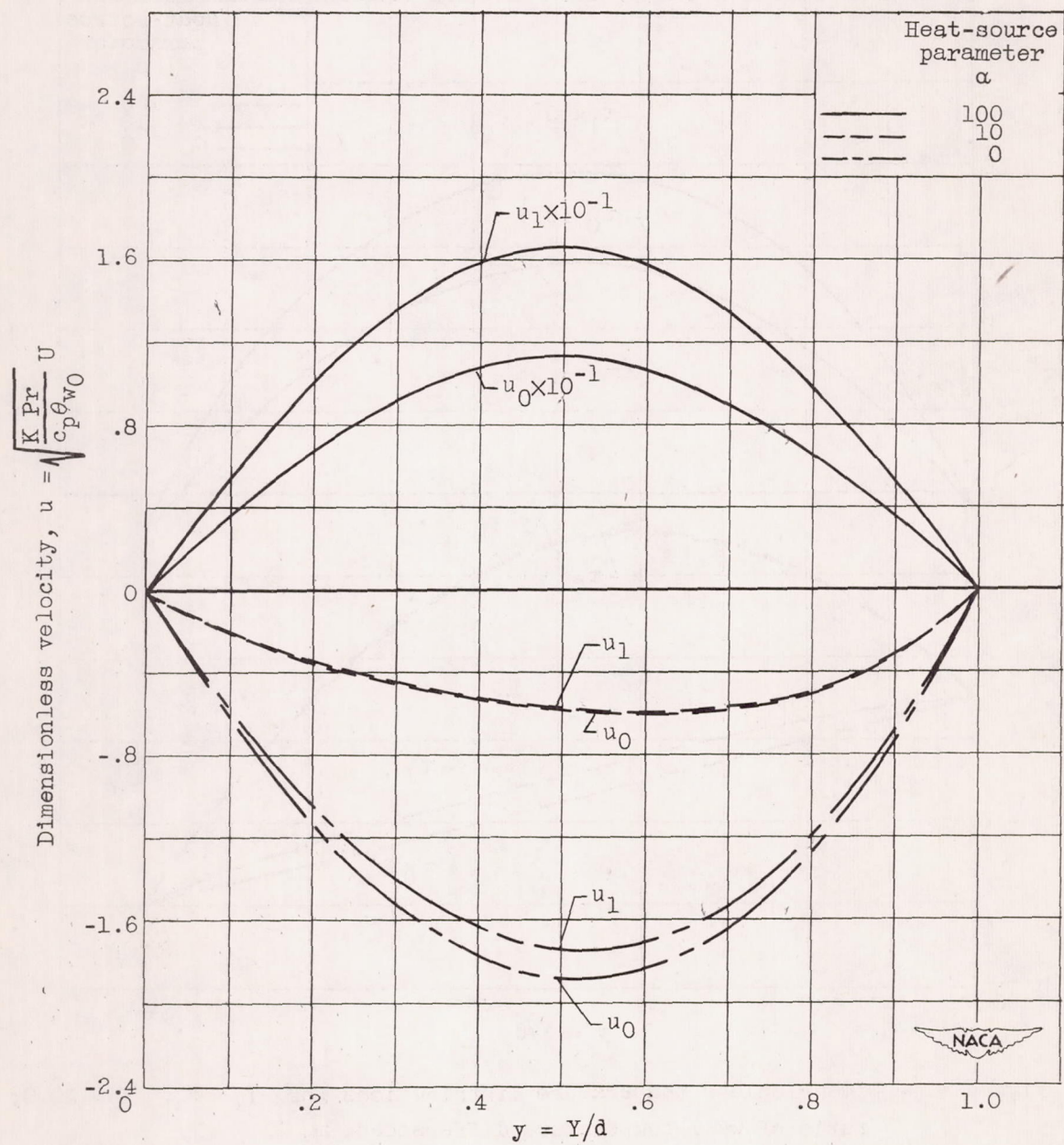


Figure 8. - Dimensionless velocity distributions for $T_w < T_s$. $K = 10.0$; ratio of wall-temperature differences, m , 2.

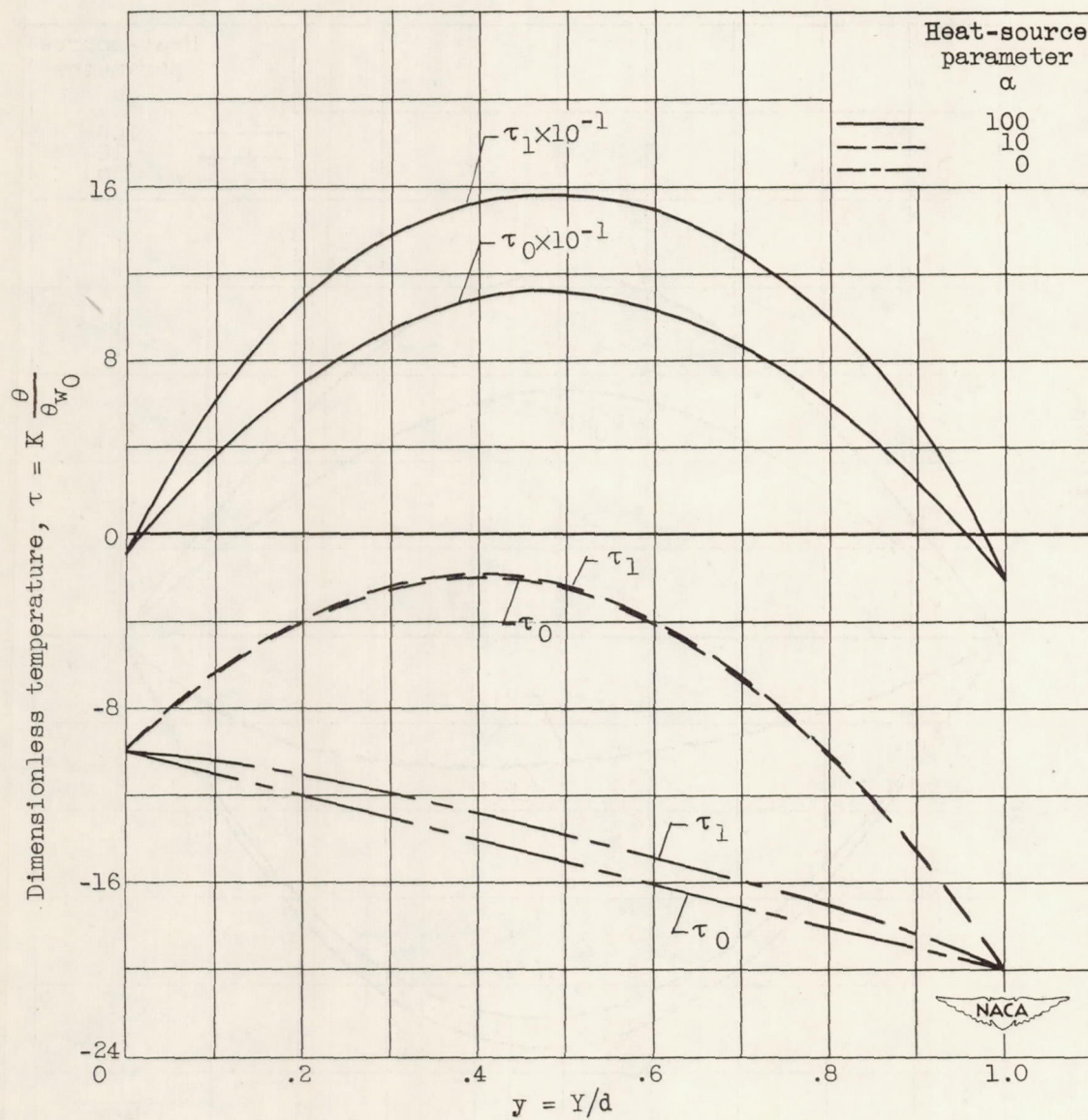


Figure 9. - Dimensionless temperature distributions for $T_w < T_s$. $K = 10.0$; ratio of wall-temperature differences, m , 2.

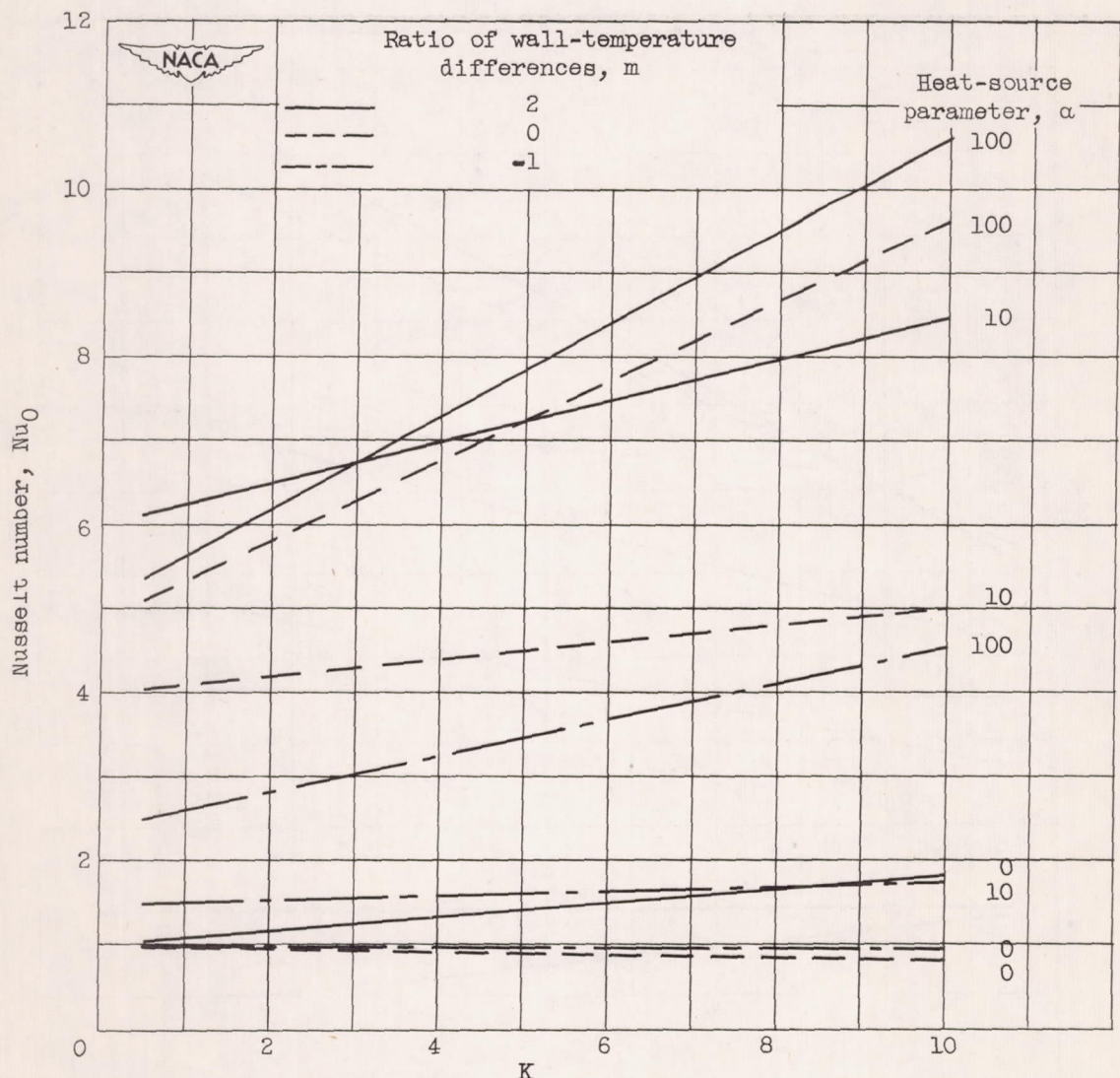


Figure 10. - Nusselt number for wall at $y = 0$ for ratio of wall-temperature differences m of -1, 0, and 2. Curves for $\alpha = 100$ are plotted for one-tenth actual value.

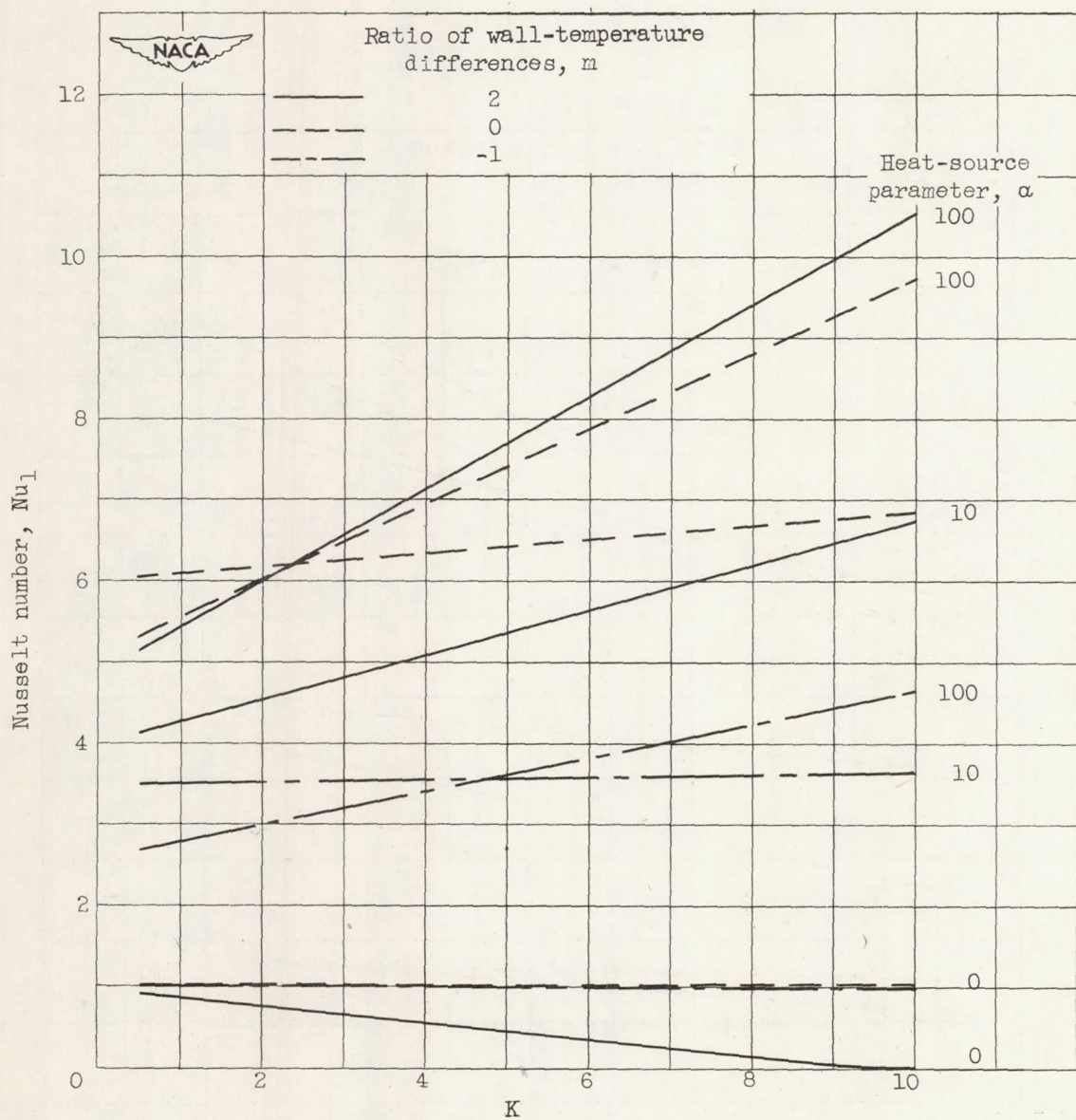


Figure 11. - Nusselt number for wall at $y = 1$ for ratio of wall-temperature differences m of -1, 0, and 2. Curves for $\alpha = 100$ are plotted for one-tenth actual value.

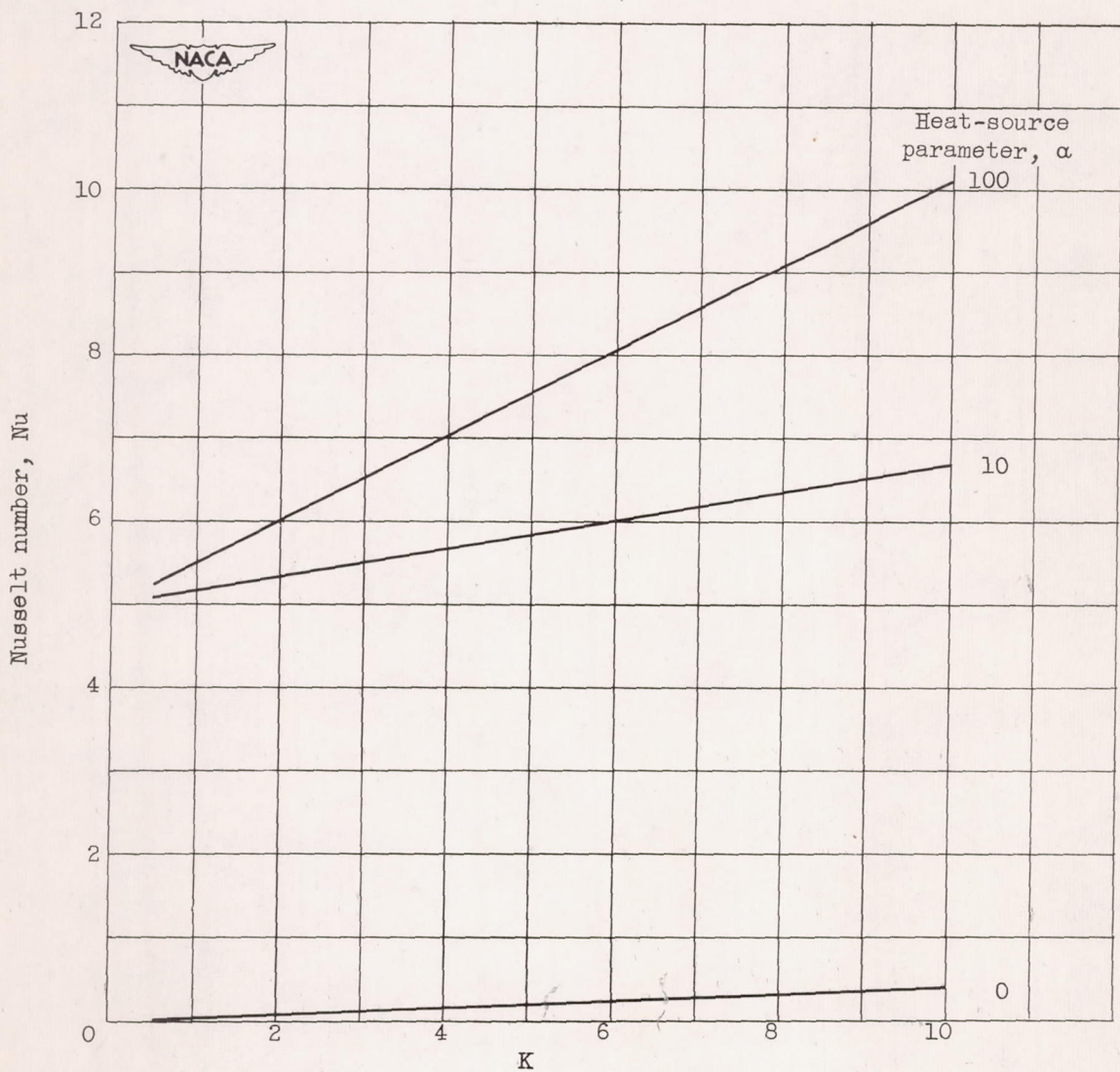


Figure 12. - Nusselt number for walls at same temperature ($m = 1$).

